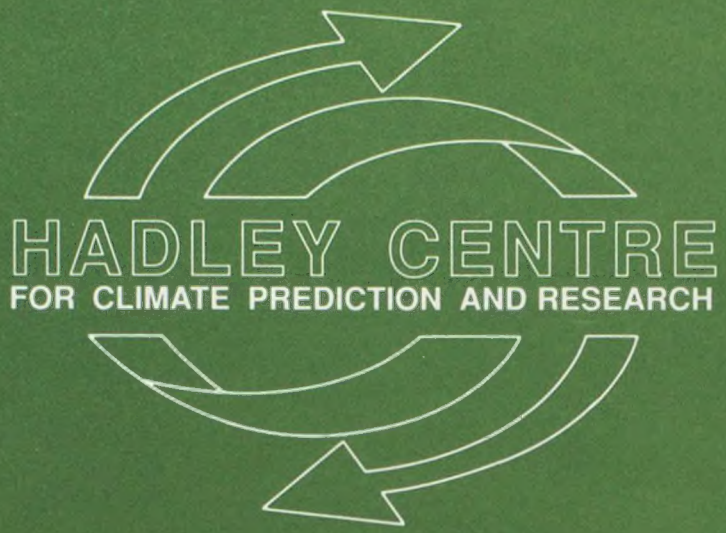

Intraseasonal variability of the Indian summer monsoon simulated by the Hadley Centre climate model

by

K Ashok, D Gregory and P M Inness

CRTN 60

September 1995

CLIMATE
RESEARCH
TECHNICAL
NOTE

Hadley Centre
Meteorological Office
London Road
Bracknell
Berkshire RG12 2SY

CLIMATE RESEARCH TECHNICAL NOTE NO. 60

INTRASEASONAL VARIABILITY OF THE INDIAN SUMMER MONSOON SIMULATED BY THE HADLEY CENTRE CLIMATE MODEL

by

K Ashok, D Gregory and P M Inness

Hadley Centre for Climate Prediction and Research
Meteorological Office
London Road
Bracknell
Berkshire RG12 2SY

NOTE: This paper has not been published. Permission to quote from it should be obtained from the Director of the Hadley Centre.

INTRASEASONAL VARIABILITY OF THE INDIAN SUMMER MONSOON SIMULATED BY THE HADLEY CENTRE CLIMATE MODEL

K. ASHOK*, D. GREGORY AND P.M. INNESS

HADLEY CENTRE FOR CLIMATE PREDICTION AND RESEARCH
LONDON ROAD, METEOROLOGICAL OFFICE, BRACKNELL
BERKS RG12 2SY, UK

* Permanent Affiliation : Indian Institute of Tropical Meteorology, Pune - 411 008, India.

ABSTRACT

A descriptive study of the intraseasonal variability of the Indian summer monsoon as simulated by the Hadley Centre Climate Model is presented. Time series analysis reveals that the model is able to represent the onset of the monsoon accurately and also the northward shift of the surface monsoon trough and rainfall characteristic of a break in the Indian summer monsoon. Study of an integration with a much weakened Madden-Julian oscillation shows little intraseasonal variability over India suggesting, in line with previous work, that this global oscillation is a major cause for the cycle of active and break periods of the Indian summer monsoon.

1. Introduction

The Indian Summer Monsoon is an important feature of the global circulation and has invoked a lot of interest in the meteorological community not only of India but also worldwide, both from an observational and modelling perspective. Many of the current generation of General Circulation Models (GCMs) are able to produce reasonably good mean simulations of the Indian monsoon capturing the broad scale pressure distribution and low level wind flow associated with the monsoon. However the spatial and temporal variations in rainfall over the subcontinent are often not well represented.

In recent years there has been increasing interest in how well GCMs simulate the variability of the Indian monsoon flow. Variations are observed to occur on a variety of different timescales, from decadal down to intraseasonal and synoptic. On the intraseasonal timescale the Indian summer monsoon is characterised by active and break periods. A break in the monsoon is said to occur when the axis of the monsoon trough shifts northwards to the foothills of the Himalayas. During such a period, rainfall decreases over central India whilst increasing over the foothills of the Himalayas, north east India also at times over Tamilnadu and Rayalaseema at the tip of south east coast of the sub-continent. A typical break lasts for 5 days but instances of prolonged breaks of 15 days duration have been recorded. Figure 1 shows typical observed monsoon break p_{msl} patterns and their departure from the long term normal pattern.

Observational studies suggest a periodicity of between 30 and 50 days for the northward propagation of rainfall over India and associated changes in wind and outgoing longwave radiation (Rama Murty, 1969; Alexander et al, 1978; Sikka and Gadgil, 1980). Because of this observed timescale several authors have suggested that break monsoon phases are related to the passage of the Madden-Julian oscillation (Madden and Julian, 1971) over the Indian region (Yasunari, 1979, Hirasawa and Yasunari,1990). Apart from these low frequency oscillations, shorter period fluctuations with periods in the range of 10-20 days are also found in rainfall. These are associated with monsoon depressions which form over the north part

of the Bay of Bengal. These track westward along the axis of the monsoon trough and give significant amounts of rainfall over the central part of India. It should be noted here that the Hadley Centre Model will not explicitly resolve such systems due to its relatively coarse grid (see section 2).

Several previous theoretical studies have attempted to understand the mechanism of the northward propagating mode (for example Keshavamurty et al, 1986). The simple model of Webster and Chou (1980) was able to produce short period active and break monsoons, based on a feedback mechanism between surface hydrology and cloudiness. However very few GCM studies have considered the intraseasonal variability of the Indian monsoon, although Goswami and Shukla (1984) using a zonally symmetric version of the GLAS model obtained low frequency oscillations.

This paper studies the intraseasonal variability of the Indian summer monsoon as simulated by the Hadley Centre Climate Model, a version of the UK Met. Office Unified Model. This model is known to be able to reasonably simulate many aspects of the Madden-Julian oscillation (Inness and Gregory, 1994) and so, if this is the dominant forcing for break and active periods, might be expected to reproduce some of the observed variability over India. The work is mainly descriptive, comparisons being made to available observations and demonstrates the current capabilities of a state of the art climate model. However some indication of the mechanisms involved in the cause of active/break monsoon behaviour is obtained by considering simulations with and without a strong Madden-Julian oscillation.

2. Model Description, Data and Methodology

The model used in this study is the Hadley Centre Climate Model, a version of the UK Met. Office Unified Model as described by Cullen (1993), being of a grid-point type with 19 (irregular) levels in the vertical using a hybrid sigma/pressure co-ordinate. A conservative split-explicit integration scheme is used (Cullen et al, 1991), and cloud water and ice are

included as prognostic variables. A horizontal resolution of 2.5°x3.75° latitude-longitude is used with a thirty minute timestep.

The annual cycle of radiation is imposed on the model which employs an interactive radiation scheme (Ingram, 1993) incorporating the cloud optical property scheme of Slingo (1989) using cloud water contents predicted by the cloud scheme of Smith (1990) (described in greater detail later). The radiation scheme is called every 3 hours in order to represent the diurnal cycle but the incoming solar flux is updated every timestep to avoid discontinuities in surface properties. The boundary layer scheme is formulated in terms of conserved variables and so can represent both dry and cloudy boundary layers (Smith, 1994). Mixing coefficients are stability dependent, using a moist Richardson number. A mass-flux convection scheme with stability dependent closure (Gregory and Rowntree, 1990) is included which includes a representation of deep convective downdraughts (Gregory and Allen, 1991). Surface hydrology and a soil temperature model are also included (Warrilow et al (1986), Dolman and Gregory (1992)). Mean orography is used together with the gravity wave drag scheme of Palmer et al (1986), although this has been modified to limit orographic variance through consideration of the Froude number of the flow rather than the original cut off of orographic variance (Wilson and Swinbank, 1991). Over the oceans the model is forced at its lower boundary with climatologically varying sea surface temperatures.

Inness and Gregory (1994) demonstrated the ability of the Hadley Centre Climate Model to represent the seasonal mean Indian monsoon circulation. In this paper the ability of the same model to capture the evolution and intraseasonal variability of the Indian monsoon is considered using two experiments. The first is a 10 year simulation with climatologically varying SSTs. Years 3 and 4 are analyzed in order to ascertain whether any intraseasonal variability simulated is characteristic of the model. The version of the model used in this simulation is similar to that used by Inness and Gregory (1994) and reproduces many of the observed features of the Madden-Julian oscillation. Figure 2(a) shows a time/longitude cross-section of 200mb velocity potential anomalies from the model averaged between 5°N and 5°S. A 20 to 70 day bandpass filter has been applied to the data to isolate variability on the

timescale of the Madden-Julian oscillation. Eastward propagating features are clearly visible with a period of 20-50 days, and the amplitude of the variability is of the same order as the observed oscillation (see Inness and Gregory (1994)).

The second experiment includes a modified convection scheme which represents the effects of convection upon horizontal momentum (Gregory et al, 1995). This only provides a crude downgradient treatment of convective momentum transports, not accounting for cloud scale pressure gradients or cloud organisation. This version of the model also provides a reasonable description of the mean structure of the Indian monsoon but only a weak incoherent Madden-Julian oscillation. Figure 2(b) shows the bandpass filtered 200mb velocity potential anomalies from a year of this experiment. There are no coherent eastward propagating features visible, and the amplitude of the variability is also much lower. A single year of this experiment is studied providing an indication as to the importance of the Madden-Julian oscillation in forcing intraseasonal variability over India.

Timeseries analysis of precipitation, low level vorticity and mean sea-level pressure was carried out to discover dominant periodicities and correlations between these parameters during the Indian summer monsoon. For this purpose the area between 65°E to 93°E and 0°N to 30°N was defined as the Indian Region, being subdivided in to two parts; S. India (65°E to 93°E and 0°N to 20°N) and N. India (65°E to 93°E, 20°N to 30°N) (fig 3), in order to study break monsoon behaviour. In the precipitation timeseries, a mask has been applied to ocean areas so that only rainfall over land areas is included in the averaging process. All the timeseries are from 1st May to 1st October. The evolution of the spatial distribution of mean sea level pressure and precipitation over the Indian region through a typical break cycle of the monsoon as simulated by the model are also considered and compared to observations.

3. Simulations of Intraseasonal Variability over India by the Hadley Centre Climate Model.

The mean simulation of the Indian summer monsoon by the Hadley Centre Climate Model has been described in some detail by Inness and Gregory (1994). Since the introduction of convective scale downdraughts (Gregory and Allen, 1991) the simulation of mean sea-level pressure, low level winds and rainfall has compared favourably with observations, although it is noted that the low level jet extends too far into the west Pacific associated with an east-west trough and excessive precipitation.

Because of this previous work only the variability of the monsoon simulation is considered here. Results are presented for the 3rd year of a 10 year simulation and both the onset and break monsoon characteristics are considered. The variability over India in the 4th year shows similar characteristics and these are also briefly discussed.

3.1 Simulation of Monsoon Onset

Figure 4 shows a sequence of simulated outgoing longwave radiation (OLR) from year 3 of the standard simulation through the period of monsoon onset, determined by consideration of the precipitation timeseries of figure 7. Deviations of OLR from $240Wm^{-2}$ are shown. Kripalani et al (1991) show that OLR values between 220 and $240Wm^{-2}$ are associated with a rainfall probability of 0.7-0.8, for rainfall greater than 2.5mm/day and OLR less than $180Wm^{-2}$ a probability of 0.9 for rainfall greater than the same value. Hence the zero line can be associated with the approximate boundary of precipitating clouds and $-60Wm^{-2}$ with deep convection. These correlations are based upon observations and so care must be exercised when applying them precisely to simulated OLR, which due to model systematic errors may not show the same correlation with precipitation. However study of the evolution of precipitation through the onset (not shown) indicated that the use of the deviation of OLR from $240Wm^{-2}$ does provide an indication of how the onset of monsoon precipitation occurs.

By the 21st of May (fig 4(d)) the monsoon is established over Kerala at the southern tip of India and by the 27th (fig 4(f)) most of the southern peninsula and the north east of India is covered by cloud. Further northward progression occurs and by the 6th of June (fig 4(i)) clouds have reached the Gujarat coast (north west India). Hence a delay of 15 days in monsoon onset is seen between the south most tip of India and the north west of the country, a figure in good agreement with observations. Figure 5 shows a sequence of composite observations of the deviation of OLR from 240Wm^{-2} (from Soman and Kumar, 1993) for the monsoon onset period. This shows a 15 day interval for precipitation to extend from the south most part of India to the north west part of the sub-continent. Hence the sequence of model simulated OLR is in good agreement with observations, although absolute values appear to be lower than observed.

3.2 Simulation of Breaks in the Monsoon

Together with the rapid increase in precipitation over India during the onset phase of the monsoon, time series of precipitation averaged over south, north and all India (Fig 6, with a 5 day running mean applied) show large variability through the monsoon season. For example, in late June into early July, rainfall over the south of India decreases by 50%. During the same period over northern India, rainfall is seen to increase. This apparent shift in rainfall from south to north India and back again is seen in other parts of the timeseries, for example in mid-July and late September.

The fluctuations in precipitation are well correlated with 850mb vorticity (fig7, with a 5 day running mean applied). Correlation coefficients between the two timeseries of precipitation and low level vorticity are high for each of the domains studied (table 1).

Region (see fig 3)	Correlation between precipitation and 850mb vorticity
South India	0.45
North India	0.58
All India	0.70

Table 1 Correlation between Rainfall and Vorticity

Increases in cyclonic vorticity over north India are associated with increased precipitation in this region and decreases further south. This may be interpolated as a northward shift of the location of the monsoon trough, with the flow becoming more zonal over the south of India, typical of break conditions.

Variations in p_{msl} are also seen (fig 8, 5 day running mean applied) which are consistent with the above interpretation. During late June pressure rises over the south of India, falling over the north associated with increased precipitation over the region.

In order to gain a fuller picture of this evolution, figure 9 presents a sequence of p_{msl} charts for the Indian region through the period of late June into early July for year 3 of the standard simulation from which the timeseries were derived. On the 20th of June (fig 9a) the trough occupies its usual position, extending from northwest India into the head of the Bay of Bengal. At 30°N a weaker zonal trough is seen over the Himalayas (to the east of 90°E) with a ridge further north. The situation on the 23rd (fig 9b) is similar, but pressure has risen in the mid-trough region over central India. By the 26th, a break pattern is established with the trough over the sub-continent shifting northward to merge with the weaker pre-existing trough near 30N and the flow over the south of India becoming more zonal. This trough continues to intensify through the end of June (fig 9d) and also moves further northwards (2nd of July,

fig 9e). By the 2nd of July, indications of trough re-establishment over central India are seen (85°E, 20°N) and by the 5th (fig 9f) the trough has been re-established in the location seen during the active phase of the monsoon. The difference in p_{msl} of a typical break day (28th June of year 3) from a normal day of active monsoon over India (20th June of year 3) is shown in fig 10. This agrees fairly well with the pattern of figure 1, the observed p_{msl} anomaly, with falls in pressure over north India and the Himalayas, and rises over the centre of the country. The falls in pressure over the Himalayas are larger than observed, but at such high elevations, algorithms to interpolate surface pressure to mean sea level must be treated with caution.

The sequence of rainfall (greater than 5mm/day) for the corresponding period is shown in figure 11. On the 20th of June (fig 11a) an active monsoon circulation exists with rainfall greater than 10mm/day being located south of 25°N over India. No rainfall greater than 5mm/day is found north of this latitude over most of the sub-continent. As the break circulation develops, rainfall over south India decreases whilst increasing in the north. By the 29th of June (fig 11d) maximum rainfall is seen north of 25°N with little of southern India having rainfall greater than 5mm/day. As the active monsoon is re-established, rainfall rates south of 25°N increase (5th July, fig 11f)

Shown in figure 12 is a sequence of 200mb velocity potential and divergent winds for the same period as figures 10 and 11. A 20 to 70 day bandpass filter has been applied to the data to isolate the intraseasonal variability. On the 20th of June, the main divergent centre in the Indian Ocean sector is located over the Bay of Bengal. In the subsequent plots, this centre moves eastward towards the Phillippines. This eastward shift of positive velocity potential from the Indian Ocean to the West Pacific sector is a signature of the Madden-Julian oscillation and its occurence at this time may be a contributory factor to the development of the monsoon break. A similar event occurs in July when there is a marked decrease in rainfall over South India, accompanied by an increase in the north Indian region. Figure 13 shows a sequence of precipitation over the Indian Ocean sector through this period, and figure 14 shows the corresponding 200mb velocity potential anomalies. On the 17th of July, the

velocity potential field in the Indian Ocean sector is dominated by a large positive anomaly south of the equator at about 100°E, but there is also a weak positive centre over the head of the Bay of Bengal. Once again, this appears to move eastwards to be centred over the north Phillippine Sea by the 23rd of July and in the west Pacific by the 2nd of August. The sequence of rainfall over India through this period is similar to that which occurs through the second half of June, described above. On the 17th of July, the rainfall over India is normal, although the east coast around 15°N is rather dry. There is then a reduction of rainfall over southern and central India on the 23rd through to the 26th, accompanied by a large increase over the Himalayan foothills on the 26th. By the 2nd of August, rainfall over most of India (except the east coast) has returned to values greater than 5mm/day.

Similar breaks in Indian monsoon activity occur in other years of the integration. Figure 15 shows rainfall over all India and also sub-divided into north and south India between the 1st of May and 1st of October for year 4 of the standard integration. During this year onset appears to be later than in year 3, rainfall not exceeding 10mm/day over northern India until late in June, although significant amounts of rainfall over Southern India from the 10th of May onwards are seen in the sequence. An example of a break in this year of the simulation is seen in mid-July when rainfall falls from over 10mm/day to 3mm/day over Southern India whilst increasing from 7 to 11mm/day over north India. This is associated with a northward shift of low level cyclonic vorticity and reduction if p_{msl} over Northern India similar to those described previously.

Spectral analysis of the precipitation and vorticity timeseries of figures 5 and 6 provide some evidence for the periodicity of the oscillation (fig 16(a) and 16(b)). Rainfall fluctuations over the south of India show a broad range of periodicities, from synoptic to intraseasonal. Over north India longer periods are dominant, with power being greatest at 37.5 days. Low level vorticity timeseries show similar periodicities. Over south India peaks occur at 25,17 and 12.5 days. For north India, peaks at 19 and 12.5 days are also seen but there is a strong peak at intraseasonal timescales (37.5 days). These periodicities are similar to the range of 20-50 days seen in a variety of observational studies during the Indian summer monsoon months.

4. Cause of break monsoon behaviour.

The standard integration above has shown that the Hadley Centre Climate Model appears able to simulate active and break monsoon periods. Inness and Gregory (1994) have shown that the model also well simulates the strength and period of the Madden-Julian oscillation. In previous observational studies several authors have suggested a link between the passage of the Madden-Julian oscillation over the Indian region and breaks in the Indian summer monsoon (e.g. Yasunari, 1979). The good simulation of active and break periods in a model with a strong Madden-Julian oscillation would tend to provide some support for these observations.

To investigate this link further a parallel integration was studied in which the convection scheme was allowed to transport horizontal momentum in the vertical. Although some aspects of the Indian monsoon simulation were improved, for example a reduction of the excessive westerly flow over the west Pacific, pressure in the monsoon trough over India was 4mb higher and the intensity of the Madden-Julian oscillation was much reduced. This latter feature of this integration allows the importance of the Madden-Julian oscillation in intraseasonal variability over India to be assessed. Figure 2(b) shows a Hovmüller diagram of 200mb velocity potential anomalies from this experiment, comparable to that shown in fig.2(a) from the control integration. In the convective momentum transport integration, there are no coherent eastward propagating disturbances and the amplitude of the variability is also clearly reduced.

Figures 17 and 18 show precipitation and 850mb vorticity timeseries for year 3 of the integration including convective momentum transports, between the 1st of May and the 1st of October. Although similar changes of low level vorticity between north and south India are seen (for example in early July) no signal is seen in rainfall. Rainfall increases rapidly in late June/early July over north India, but only a relatively small decrease in rainfall is found over South India. In the standard integration with a strong Madden-Julian oscillation

the magnitude of rainfall changes between north and south India were of a similar magnitude. Spectral analysis of the rainfall time series over north and south Indian shows no significant peak at intraseasonal periods associated with the Madden-Julian oscillation (around 50 days, not shown). Study of a sequence of surface charts for this period (fig 19) shows no northward movement of the trough, which remains approximately in the same location undergoing periodic strengthening and weakening.

Hence, although variations of precipitation and vorticity over India are found in this integration, the cycle of active and break phases of the Indian summer monsoon is poorly represented. If such variability is linked to the Madden-Julian oscillation then this would be expected as this version of the model does not simulate this feature of the tropical circulation well. Hence these results provide further support for the hypothesis that monsoon breaks occur due to the passage of the Madden-Julian oscillation over the Indian region.

5. Discussion

The variability of the circulation of the summer Indian monsoon as simulated by the Hadley Centre Climate Model has been described and compared with observations. The model appears to be able to provide a good description of monsoon onset and also active and break phases of the monsoon with a northward shift of the surface pressure trough and region of intense rainfall during break periods. Much of the analysis has been carried out on a single year, although results from a subsequent year of the integration have been briefly studied, supporting the above conclusions. However analysis of further years would be needed to build a complete picture of the model's performance.

It has been noted that the model is well able to simulate the Madden-Julian oscillation which is often ascribed to be the cause of the break of the Indian summer monsoon. Consideration of a further simulation with a much weaker Madden-Julian oscillation lends support to this mechanism. Although variations in low level vorticity are found similar to those seen during

a monsoon break, no northward shift of the surface pressure trough and precipitation are found, the variation being caused by changes in the intensity of a quasi-stationary trough.

On a related point, Inness and Gregory (1994) demonstrate using an AMIP integration of the Unified Model that the strength of the Madden-Julian oscillation is related to sea surface temperature variations in the tropical Pacific. This effect may have consequences for the variability of rainfall over India during El Nino events, although this may be dominated by the effect of El Nino upon the mean monsoon strength. However given the apparent capabilities of the model this would be a topic which might be explored further with this model.

A further possible area for investigation may be the changing nature of variability as climate changes. There is much interest in the possible change of the Indian monsoon in a warmer climate forced by higher atmospheric concentrations of greenhouse gases. Variability within a monsoon season appears to be dependent upon an aspect of the global circulation, the Madden-Julian oscillation, which current GCMs have difficulty in simulating well and when found in simulations is very sensitive to the nature of the mean flow (see Inness and Gregory 1994, Slingo et al, 1994). If the nature of the mean circulation were to change in the future due to increased greenhouse forcing, then not only could a stronger monsoon result (as found in many studies of climate change) but the nature of rainfall variablity may change also. This is beyond the current scope of the work presented here but is perhaps an issue that current GCMs may now be capable of addressing.

6. Acknowledgements

This work was carried out under a collaborative program between the Hadley Centre (Bracknell, UK) and IITM (Pune, India) funded by the British Council. One of the authors (K.Ashok) thanks British council, Bombay for funding his visit to the Hadley Centre and the Director of his parent institute (IITM, Pune, India) Prof. R. N. Keshavamurty for providing

the travel support. The authors acknowledge Mr. M. K. Soman for the discussions they had on this subject.

7. References

Alexander, G., Keshavamurty, R.N., De, U.S., Chellappa, R., Das, S.K. and Pillai, P.V., 1978 : "Fluctuations of monsoon activity", Proceedings of the International Symposium on Monsoons, New Delhi, 1977. Ind. J. of Met. Hydr. and Geoph, **29**, 76-87.

Cullen, M.J.P, 1993 : "The Unified Forecast/Climate Model.", Meteor. Mag., **122**, 81-94

Cullen , M.J.P. and Davies, T., 1991 : "A conservative split-explicit integration scheme with 4th order horizontal advection.", Quart. J. Roy. Met. Soc., **117**, 993-1002

Dakshinamurti, J. and Keshavamurty, R.N., 1976 : "On oscillation of period of one month in the Indian summer monsoon". Ind. J. of Met. Hydr. and Geoph, **27**, 201-203.

Dolman, A.J. and Gregory, D., 1992 : "The parametrization of rainfall interception in GCMs.", Quart. J. Roy. Met. Soc., **118**, 455-467

Goswami, B.N. and Shukla, J., 1984 : "Quasi-periodic oscillations in the symmetric general circulation model.", J. Atmos. Sci., **41**, 20-47.

Gregory, D. and Rowntree, P.R., 1990 : "A mass flux convection scheme with representation of cloud ensemble characteristics and stability dependent closure.", Mon. Wea. Rev., **118**, 1483-1506

Gregory, D. and Allen, S., 1991 : "The effect of convective scale downdraughts upon NWP and climate simulations.", Preprints of the 9th Conf. on Numerical Weather Prediction, Oct 14-18 1991, Denver, Co., USA

Gregory, D., Kershaw, R., and Inness, P.M., 1995 : The parameterization of convective momentum transports. Part II: Single column and general circulation model tests. In preparation.

Ingram, W.J., 1993 : "Radiation.", Unified Model Documentation Paper No. 22, available from The Unified Model Librarian, FR-Div,., Meteorological Office, London Rd, Bracknell, Berks. RG12 2SX. United Kingdom.

Inness, P.M. and Gregory, D., 1994 : "Simulation of the Indian monsoon and tropical intraseasonal variability by a General Circulation Model.", Climate Research Technical Note No. 52, available from the Hadley Centre for Climate Prediction and Change, Meteorological Office, London Rd, Bracknell, Berks. RG12 2SY, UK

Keshavamurthy, R.N. and Sankar Rao, M., 1992 : "The physics of monsoons.", Pub. by Allied Publications Ltd., Bombay, India, 199pp

Keshavamurty, R.N., Kasture, S.V. and Krishna Kumar, V., 1986 : "30-50 day oscillation of the monsoon: A new theory". Beitr Phys. Atmosph, **59**, **4**, 443-454.

Kripalani, R.H., Singh S.V. and Arkin, P.A., 1991 : "Large-scale features of rainfall and outgoing longwave radiation over Indian and adjoining regions." Contrib. Atmos. Phys., **64**, 159-168.

Krishnamurti, T.N. and Subrahmanyam, D., 1982 : "The 30-50 day mode at 850 mb during MONEX.", J. Atmos. Sci., **39**, 2088-2095.

Madden, R.A. and Julian, P.R. (1971) : "Detection of 40-50 day oscillation in the zonal wind in the tropical Pacific.", J. Atmos. Sci., **28**, 702-708.

Palmer, T.N., Shutts, G.J. and Swinbank, R., 1986 : "Alleviation of systematic westerly bias in general circulation and numerical weather prediction models through orographic gravity wave drag parametrization.", Quart. J. Roy. Met. Soc., 112, **1001**-1039

Ramamurty, K., 1969 : "Breaks in the monsoon.", Forecasting Manual, Part IV, India Meteorological Department.

Sikka, D.R. and Gadgil, S., 1980 : "On the maximum cloud zone and the ITCZ over Indian longitudes during the south-west monsoon.", Mon. Wea. Rev., **108**, 1840-1853.

Slingo, A., 1989 : "A GCM parametrization for the shortwave radiative properties of water clouds.", Journ. Atm. Sci., **46**, 1419-1427

Slingo, J.M., Sperber, K.R., Boyle, J., Ceron, J-P., Dix, M., Ebisuzaki, W., Fyfe, J., Gregory, D., Gueremy, J-F., Hack, J., Harzallah, Inness, P.M., A., Kitoh, A., Lau, W., McAvaney, B., Madden, R., Matthews, A., Palmer, T., Park, C-K., Randall, D., Renno, N., Ritchie, H., 1994 : "Intraseasonal Oscillations in 15 General Circulation Models : Results from an AMIP Diagnostic Subproject.", PCMDI Report, PCMDI, Lawrence Livermore National Laboratory, California.

Smith, R.N.B., 1990 : "A scheme for predicting layer clouds and their water content in a general circulation model.", Quart. J. Roy. Met. Soc., **116**, 435-460

Smith, R.N.B., 1994 : "Experience and developments with layer cloud and boundary layer mixing schemes in the UKMO Unified Model.", Workshop on the Parametrization of the Cloud Topped Boundary Layer, 8-11 June 194, 319-340, ECMWF, Reading, Berks.

Soman, M.K. and Kumar, K., 1993 : "Space-time Evolution of Meteorological Features associated with the Onset of Indian Summer Monsoon.", Mon. Wea. Rev., **121**,1177-1193.

Warrilow, D.A., Sangster, A.B., and Slingo, A., 1986 : "Modelling land surface processes and their influence on European climate.", Dynamical Climatology Technical Note No. 38, Available fro the Hadley centre, Meterological Office, London Rd, Bracknell, Berks. RG12 2SY United Kingdom.

Webster, P.J., and Chou, L., 1980 : "Low frequency transitions of a simple monsoon system.", J. Atmos. Sci., **37**, 368-381.

Wilson, C.A. and Swinbank, R., 1991 : "Gravity wave drag.", Unified Model Documentation Paper No. 22, available from The Unified Model Librarian, FR-Div,., Meteorological Office, London Rd, Bracknell, Berks. RG12 2SX. United Kingdom.

Yasunari, T., 1979 : "Cloudiness fluctuations associated with the northern hemisphere summer monsoon.", J. Met. Soc. Japan, **57**, 227-242.

Yasunari, T., 1980 : "A quasi-stationary apperance of 30-40 day period in the cloudiness fluctuations during the summer monsoon over India.", J. Met. Soc. Japan, **58**, 225-229.

List of Figures

Figure 1. Typical p_{msl} patterns associated with break monsoon behaviour. (From Keshavamurty and Sankar Rao, 1992).

Figure 2. Time-longitude (Hovmüller) diagrams of 200mb velocity potential anomalies (m^2s^{-2}) averaged between 5°N and 5°S,. A 20-70 day bandpass filter has been applied to the data, (a) from year 3 of the standard model integration, (b) from year 3 of the integration with convective momentum transports.

Figure 3. Domains of timeseries for North and South India.

Figure 4. Sequence of outgoing longwave radiation (difference from $240Wm^{-2}$) over India at 3 day intervals through the onset of the monsoon in year 3 of the standard integration. Negative deviations from $240Wm^{-2}$ are shaded.

Figure 5. Composite sequence of outgoing longwave radiation (difference from $240Wm^{-2}$) through the onset of the Indian monsoon. (From Soman and Kumar, 1993)

Figure 6. Timeseries of simulated precipitation (mm/day) from the 1st of May to 1st of October for year 3 of a standard integration of the Hadley Centre Climate Model for (a) south India, (b) north India and (c) all India with 5 day moving average applied.

Figure 7. Timeseries of simulated 850mb vorticity (s^{-1}) from the 1st of May to 1st of October for year 3 of a standard integration of the Hadley Centre Climate Model for (a) south India, (b) north India and (c) all India with 5 day moving average applied.

Figure 8. Timeseries of simulated p_{msl} (mb) from the 1st of May to 1st of October for year 3 of a standard integration of the Hadley Centre Climate Model for (a) south India, (b) north India and (c) all India with 5 day moving average applied.

Figure 9. Sequence of p_{msl} (mb) over the Indian region at 3 day intervals for the 20th of June to 5th of July for year 3 of the standard integration illustrating the formation of a monsoon break as simulated by the Hadley Centre Climate Model.

Figure 10. Difference in p_{msl} between a break (28th June) and normal (20th June) day of the Indian monsoon for year 3 of the standard integration.

Figure 11. Sequence of precipitation distributions (mm/day) at 3 day intervals for the same period as figure 9 illustrating the pattern of rainfall behaviour during a monsoon break as simulated by the Hadley Centre Climate Model. Values greater than 15mm/day shaded.

Figure 12. Sequence of 200mb velocity potential anomalies (m^2s^{-2}) at 3 day intervals for the same period as figure 11. A 20-70 day filter has been applied to the data.

Figure 13. Sequence of precipitation distributions (mm/day) at 3 day intervals for the period 17th of July to 2nd of August. Values greater than 15mm/day shaded.

Figure 14. Sequence of 200mb velocity potential anomalies (m^2s^{-2}) at 3 day intervals for the same period as figure 13. A 20-70 day filter has been applied to the data.

Figure 15. Timeseries of simulated precipitation (mm/day) from the 1st of May to 1st of October for year 4 of a standard integration of the Hadley Centre Climate Model for (a) south India, (b) north India and (c) all India with 5 day moving average applied.

Figure16a. Spectra of timeseries of precipitation (mm/day) of figure 3 for (a) south India, (b) north India and (c) all India

Figure 16b. Spectra of timeseries of 850mb vorticity (s^{-1}) of figure 4 for (a) south India, (b) north India and (c) all India

Figure 17. Timeseries of simulated 850mb vorticity (s^{-1}) from the 1st of May to 1st of October for year 3 of an integration of the Hadley Centre Climate Model including the transport of horizontal momentum by convection for (a) south India, (b) north India and (c) all India with 5 day moving average applied.

Figure 18. Timeseries of simulated precipitation (mm/day) from the 1st of May to 1st of October for year 3 of an integration of the Hadley Centre Climate Model including the transport of horizontal momentum by convection for (a) south India, (b) north India and (c) all India with 5 day moving average applied.

Figure 19. Sequence of p_{msl} (mb) over the Indian region at 3 day intervals for the 20th of June to 5th of July for year 3 of an integration of the Hadley Centre Climate Model including the horizontal transport of momentum by convection.

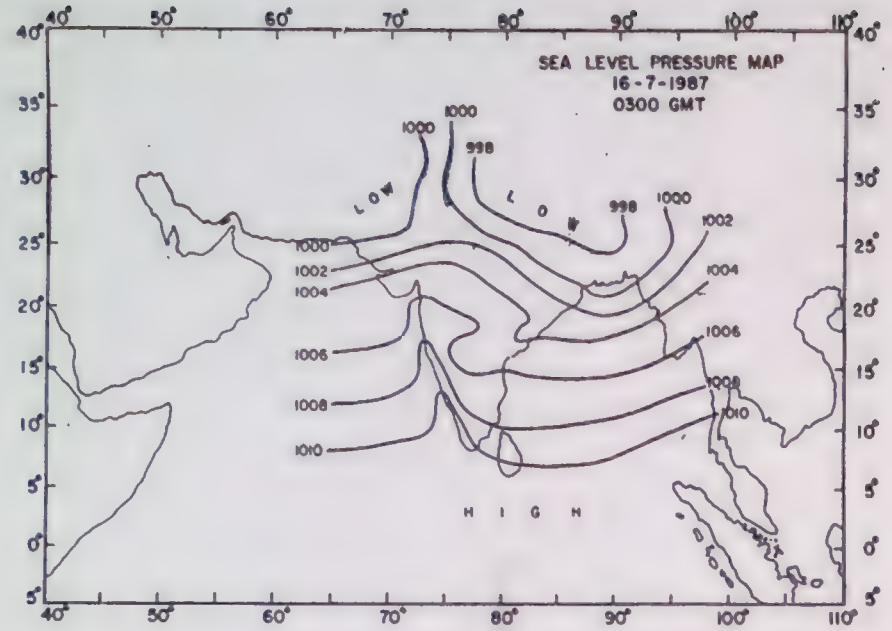
SEA LEVEL PRESSURE MAP
16-7-1987
0300 GMT
LOW
LOW
HIGH
1000
998
1002
1004
1006
1008
1010

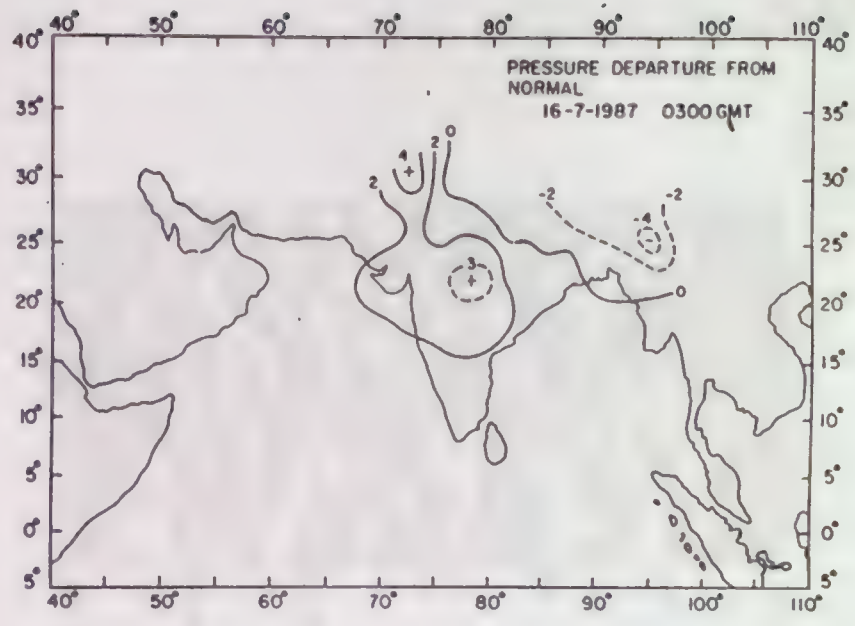
PRESSURE DEPARTURE FROM
NORMAL
16-7-1987 0300 GMT

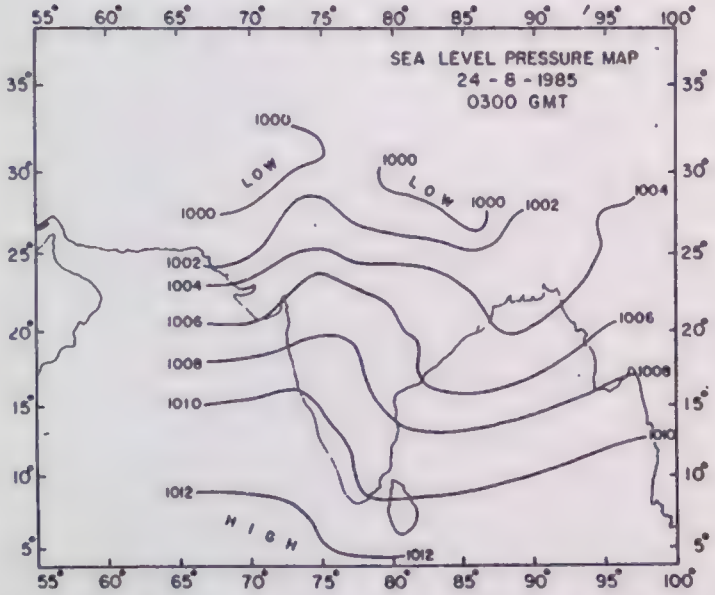
SEA LEVEL PRESSURE MAP
24-8-1985
0300 GMT
LOW
LOW
HIGH
1000
1002
1004
1006
1008
1010
1012

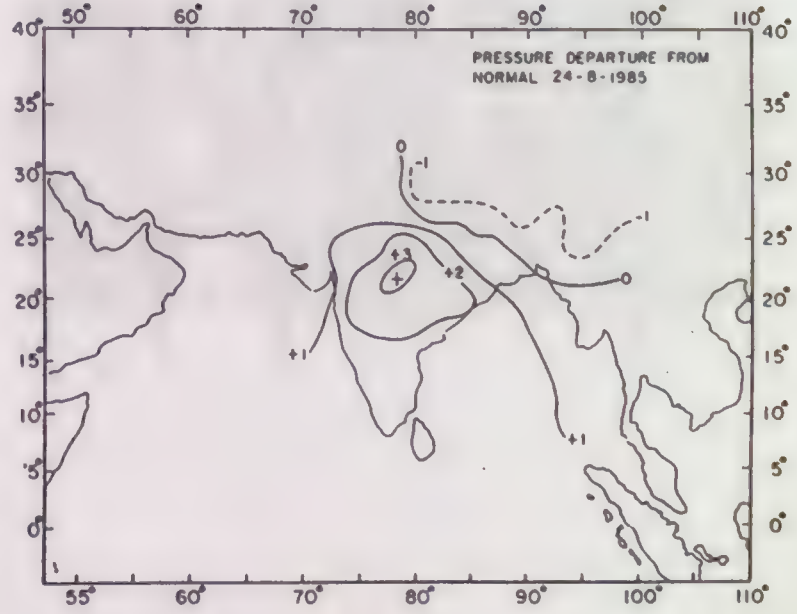
PRESSURE DEPARTURE FROM
NORMAL 24-8-1985

Figure 1

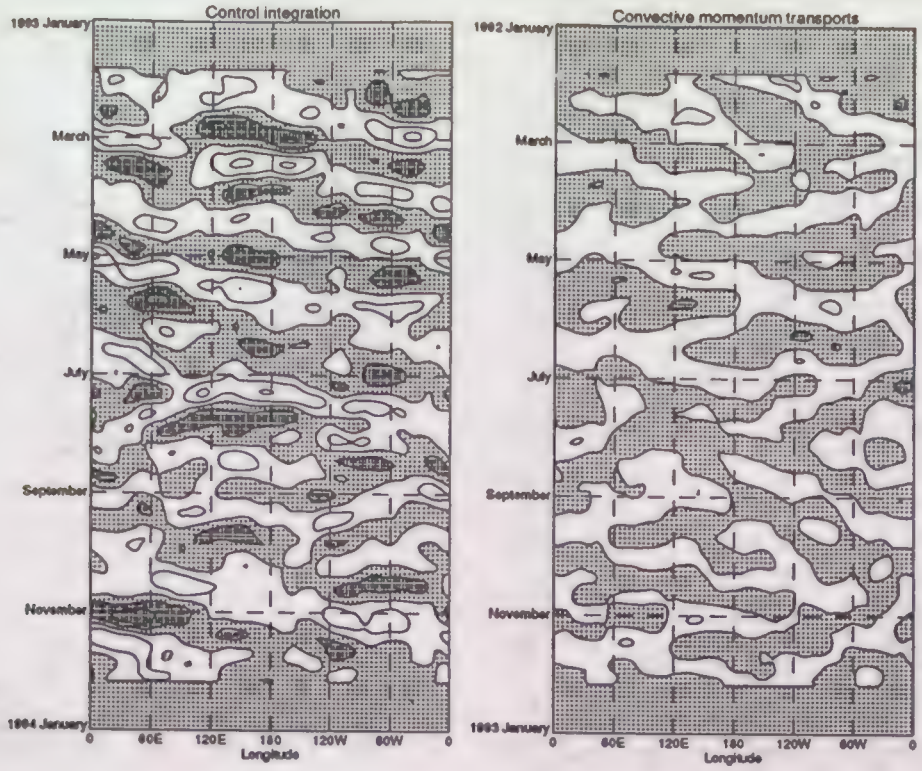
Control integration
1993 January
March
May
July
September
November
1994 January
0
60E
120E
180
120W
60W
0
Longitude
Convective momentum transports
1992 January
March
May
July
September
November
1993 January
0
60E
120E
180
120W
60W
0
Longitude

(a) (b)

Figure 2

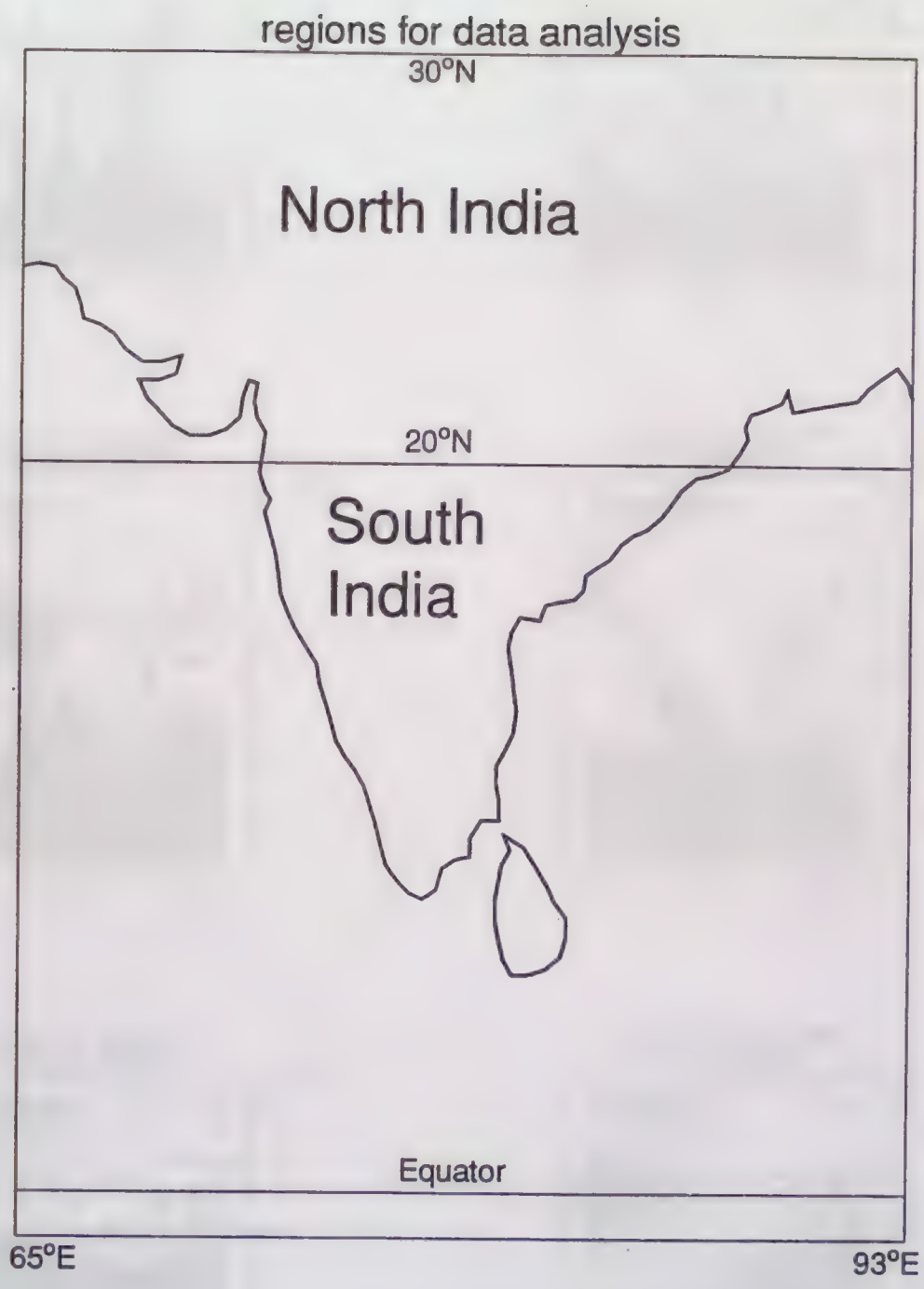
regions for data analysis
30°N
North India
20°N
South
India
Equator
65°E
93°E

Figure 3

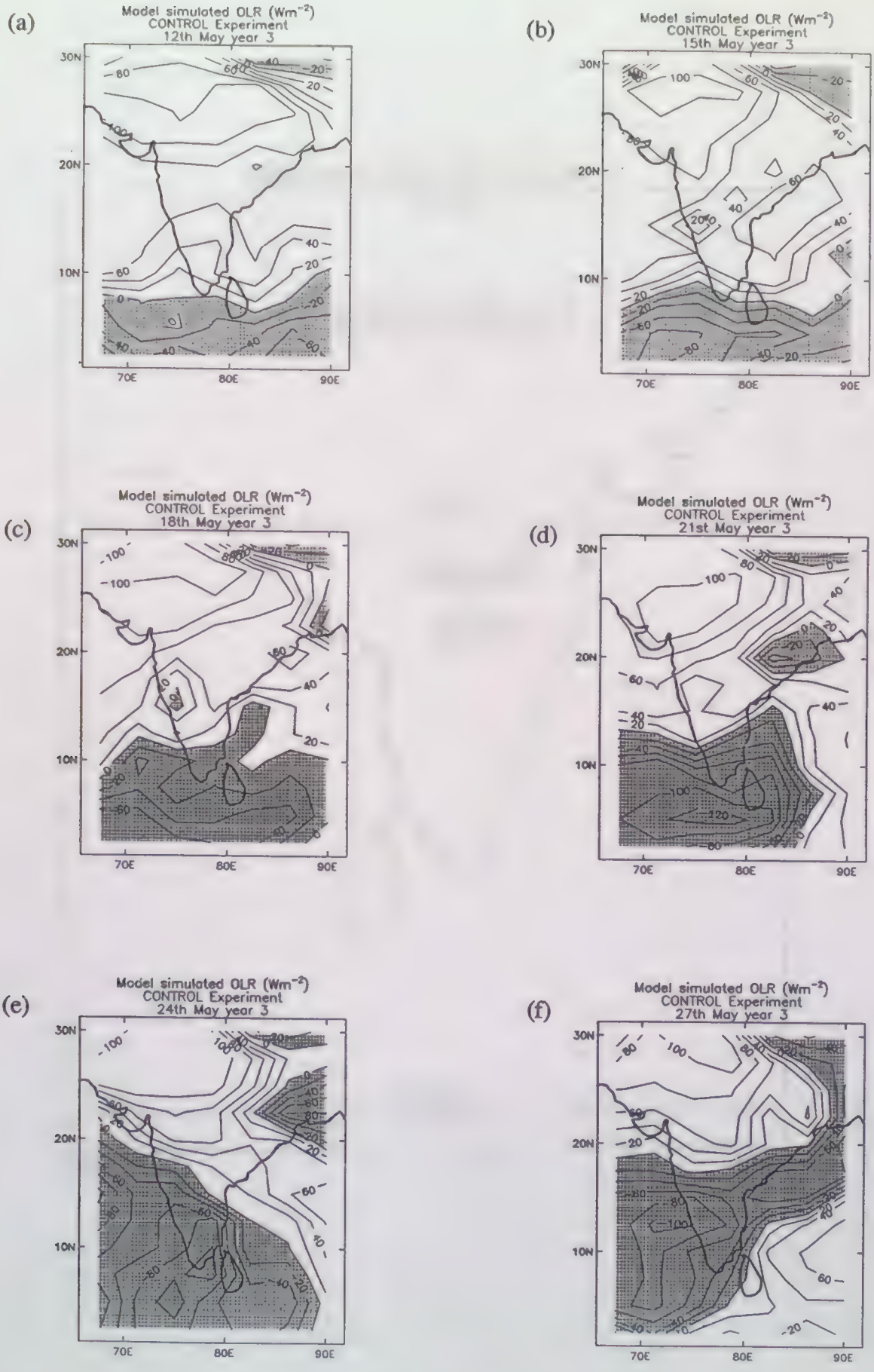
(a)
Model simulated OLR (Wm^{-2})
CONTROL Experiment
12th May year 3
(b)
Model simulated OLR (Wm^{-2})
CONTROL Experiment
15th May year 3
(c)
Model simulated OLR (Wm^{-2})
CONTROL Experiment
18th May year 3
(d)
Model simulated OLR (Wm^{-2})
CONTROL Experiment
21st May year 3
(e)
Model simulated OLR (Wm^{-2})
CONTROL Experiment
24th May year 3
(f)
Model simulated OLR (Wm^{-2})
CONTROL Experiment
27th May year 3
30N
20N
10N
70E
80E
90E

Figure 4

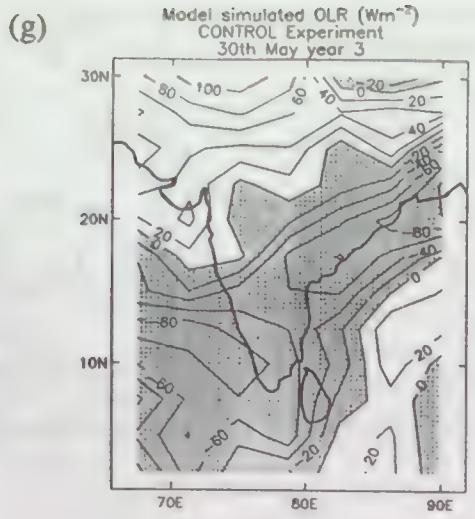

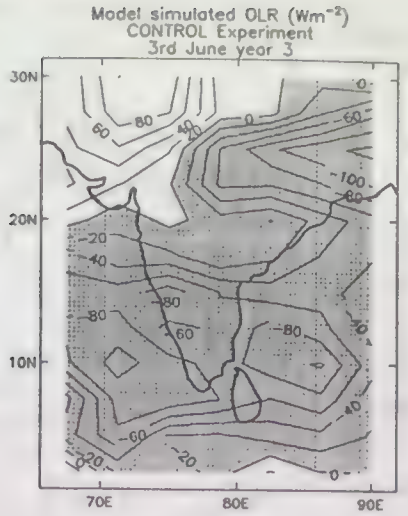

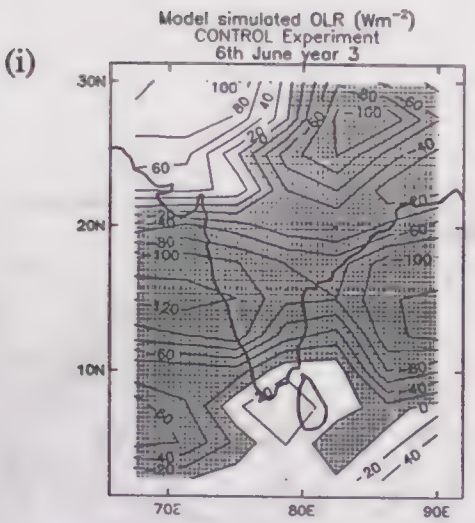

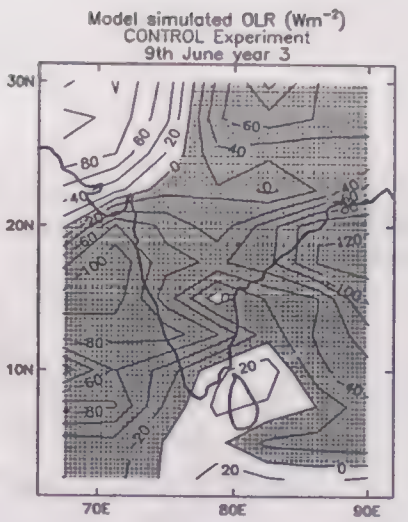

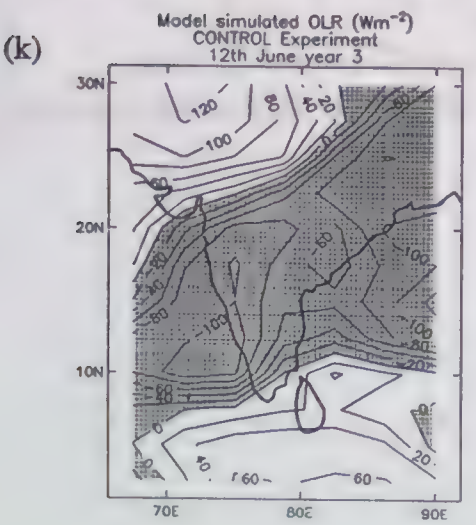

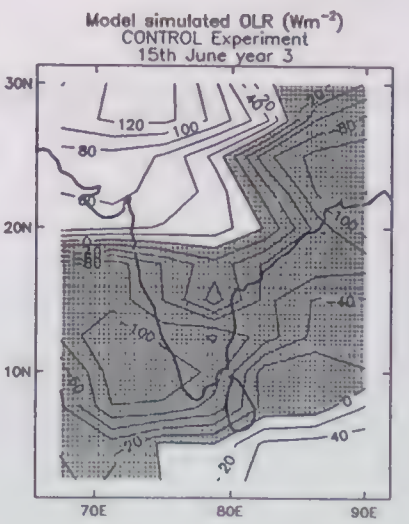

Figure 4 contd.

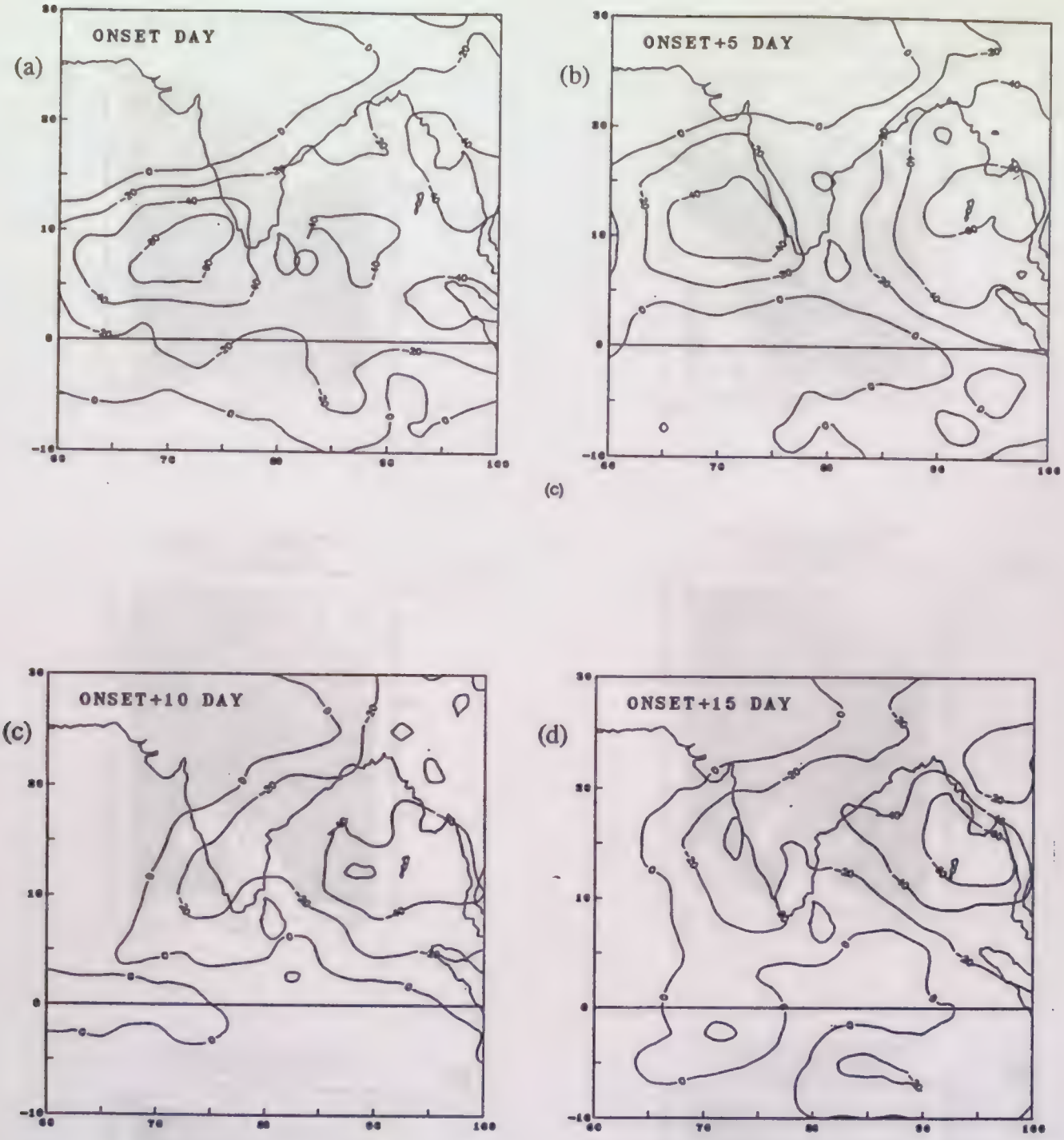

Figure 5

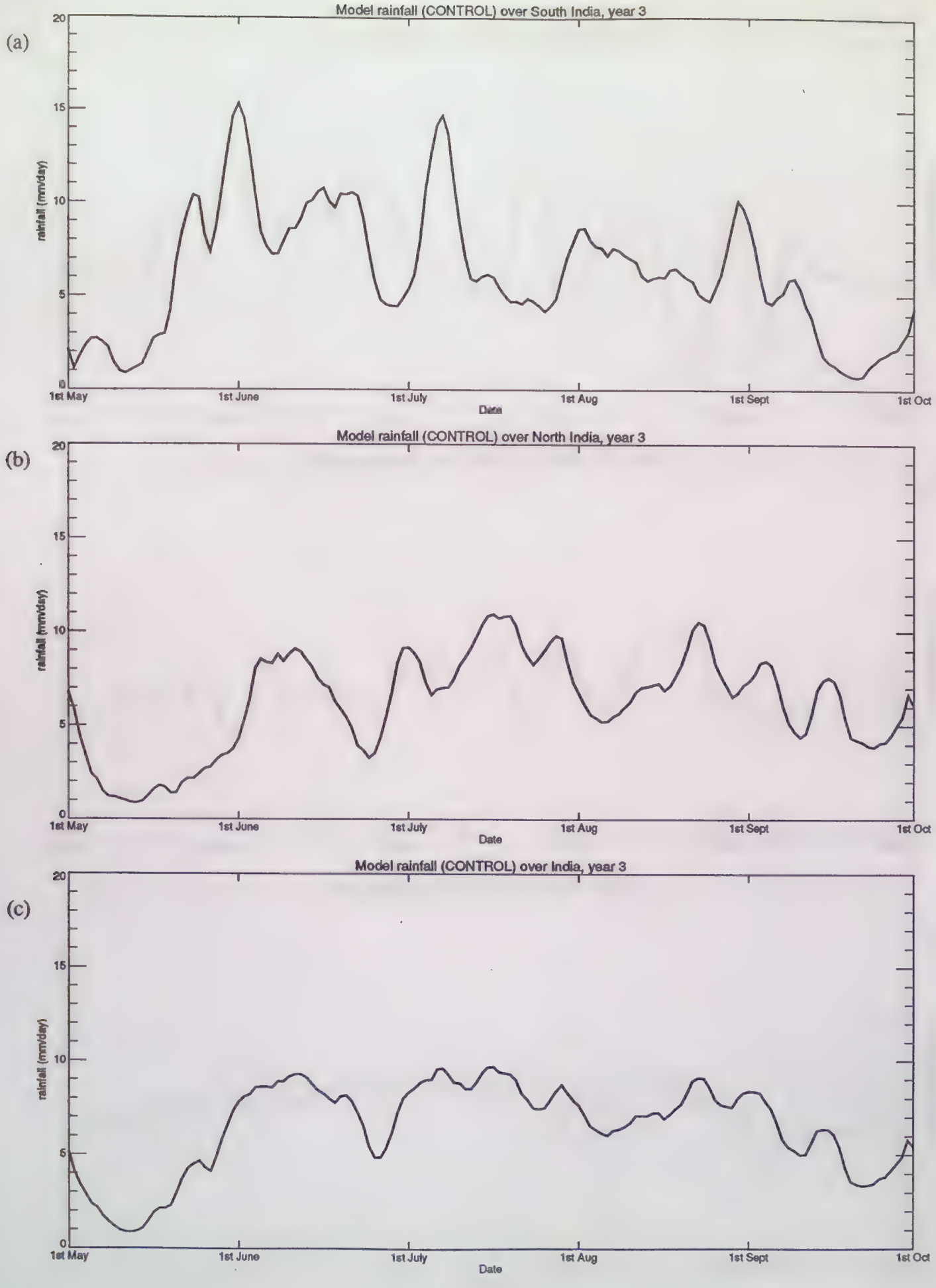
(a)
Model rainfall (CONTROL) over South India, year 3
rainfall (mm/day)
20
15
10
5
0
1st May
1st June
1st July
1st Aug
1st Sept
1st Oct
Date
(b)
Model rainfall (CONTROL) over North India, year 3
rainfall (mm/day)
20
15
10
5
0
1st May
1st June
1st July
1st Aug
1st Sept
1st Oct
Date
(c)
Model rainfall (CONTROL) over India, year 3
rainfall (mm/day)
20
15
10
5
0
1st May
1st June
1st July
1st Aug
1st Sept
1st Oct
Date

Figure 6

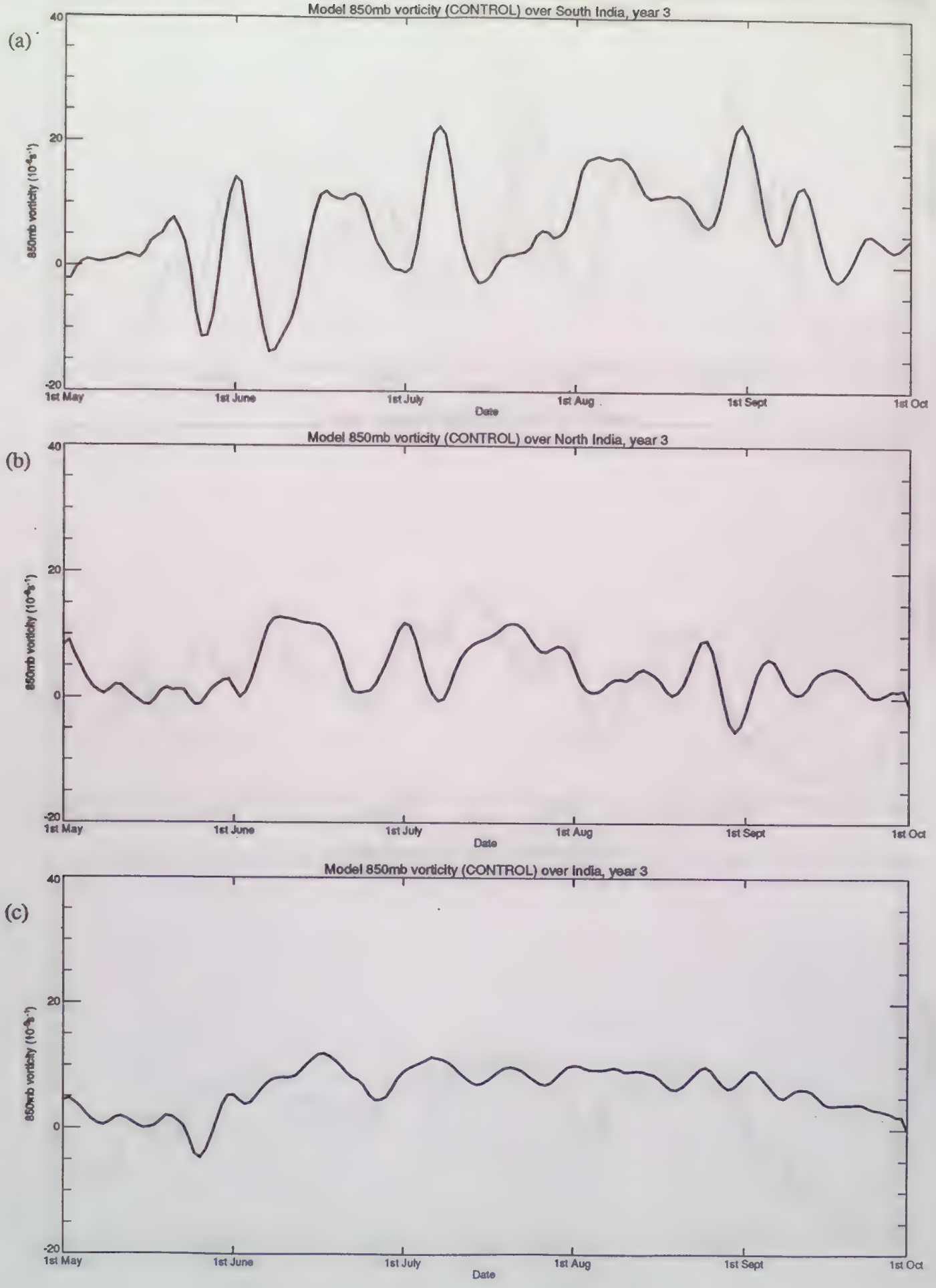
(a)
Model 850mb vorticity (CONTROL) over South India, year 3
850mb vorticity (10⁻⁶s⁻¹)
40
20
0
-20
1st May
1st June
1st July
1st Aug
1st Sept
1st Oct
Date
(b)
Model 850mb vorticity (CONTROL) over North India, year 3
850mb vorticity (10⁻⁶s⁻¹)
40
20
0
-20
1st May
1st June
1st July
1st Aug
1st Sept
1st Oct
Date
(c)
Model 850mb vorticity (CONTROL) over India, year 3
850mb vorticity (10⁻⁶s⁻¹)
40
20
0
-20
1st May
1st June
1st July
1st Aug
1st Sept
1st Oct
Date

Figure 7

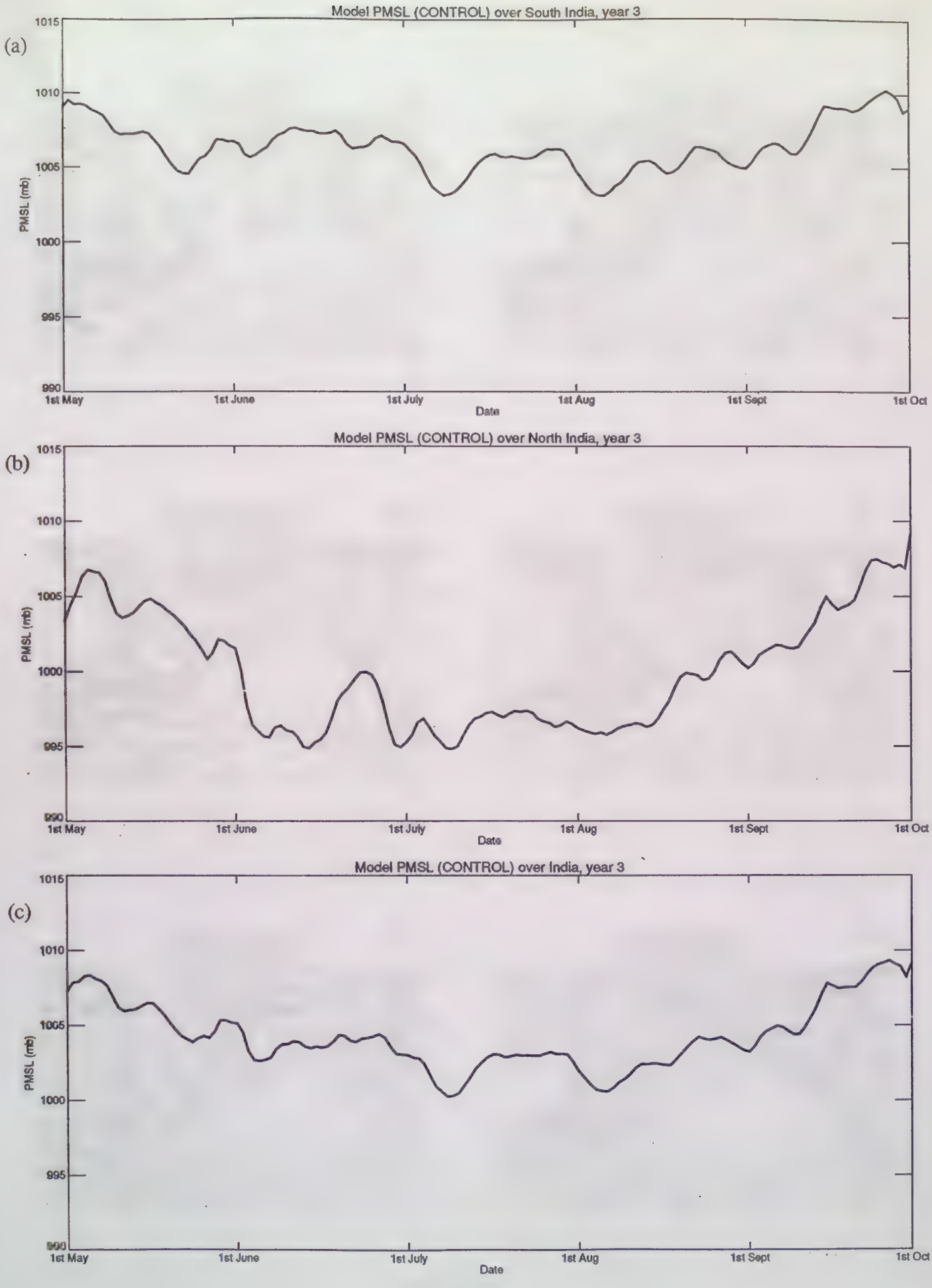
(a)
Model PMSL (CONTROL) over South India, year 3
PMSL (mb)
1015
1010
1005
1000
995
990
1st May
1st June
1st July
1st Aug
1st Sept
1st Oct
Date
(b)
Model PMSL (CONTROL) over North India, year 3
PMSL (mb)
1015
1010
1005
1000
995
990
1st May
1st June
1st July
1st Aug
1st Sept
1st Oct
Date
(c)
Model PMSL (CONTROL) over India, year 3
PMSL (mb)
1015
1010
1005
1000
995
990
1st May
1st June
1st July
1st Aug
1st Sept
1st Oct
Date

Figure 8

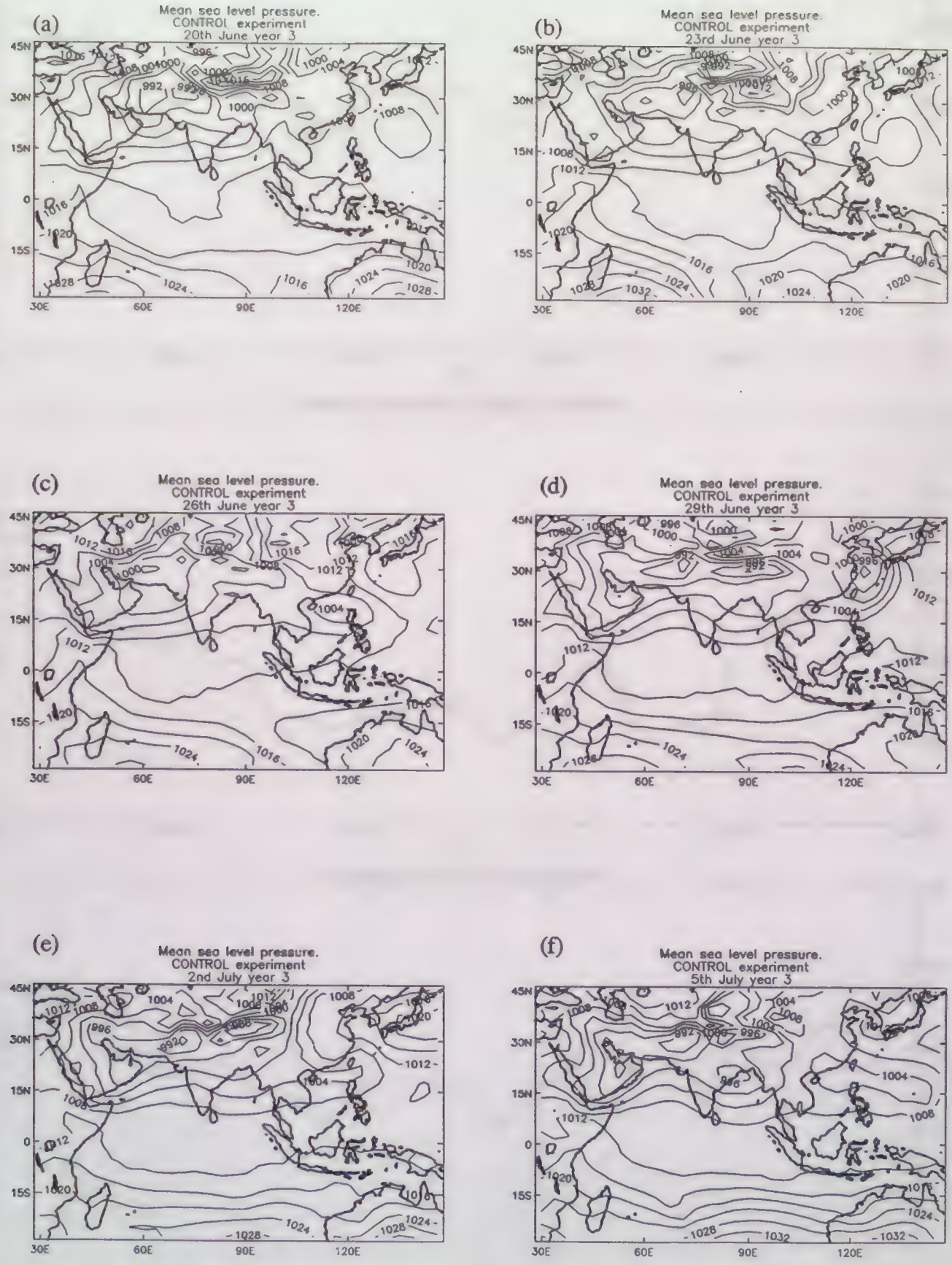
(a)
Mean sea level pressure.
CONTROL experiment
20th June year 3
(b)
Mean sea level pressure.
CONTROL experiment
23rd June year 3
(c)
Mean sea level pressure.
CONTROL experiment
26th June year 3
(d)
Mean sea level pressure.
CONTROL experiment
29th June year 3
(e)
Mean sea level pressure.
CONTROL experiment
2nd July year 3
(f)
Mean sea level pressure.
CONTROL experiment
5th July year 3
45N
30N
15N
0
15S
30E
60E
90E
120E

Figure 9

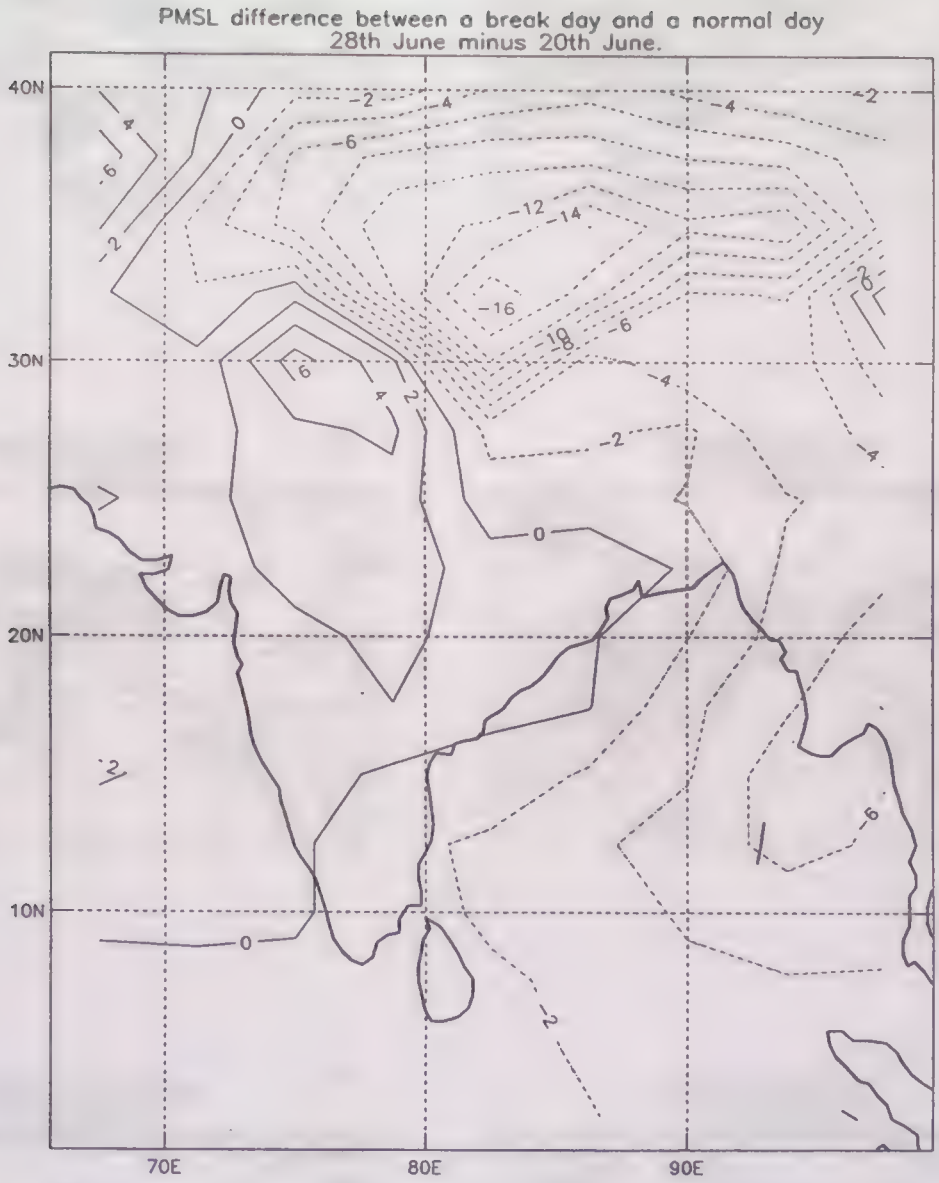
PMSL difference between a break day and a normal day
28th June minus 20th June.
40N
30N
20N
10N
70E
80E
90E

Figure 10

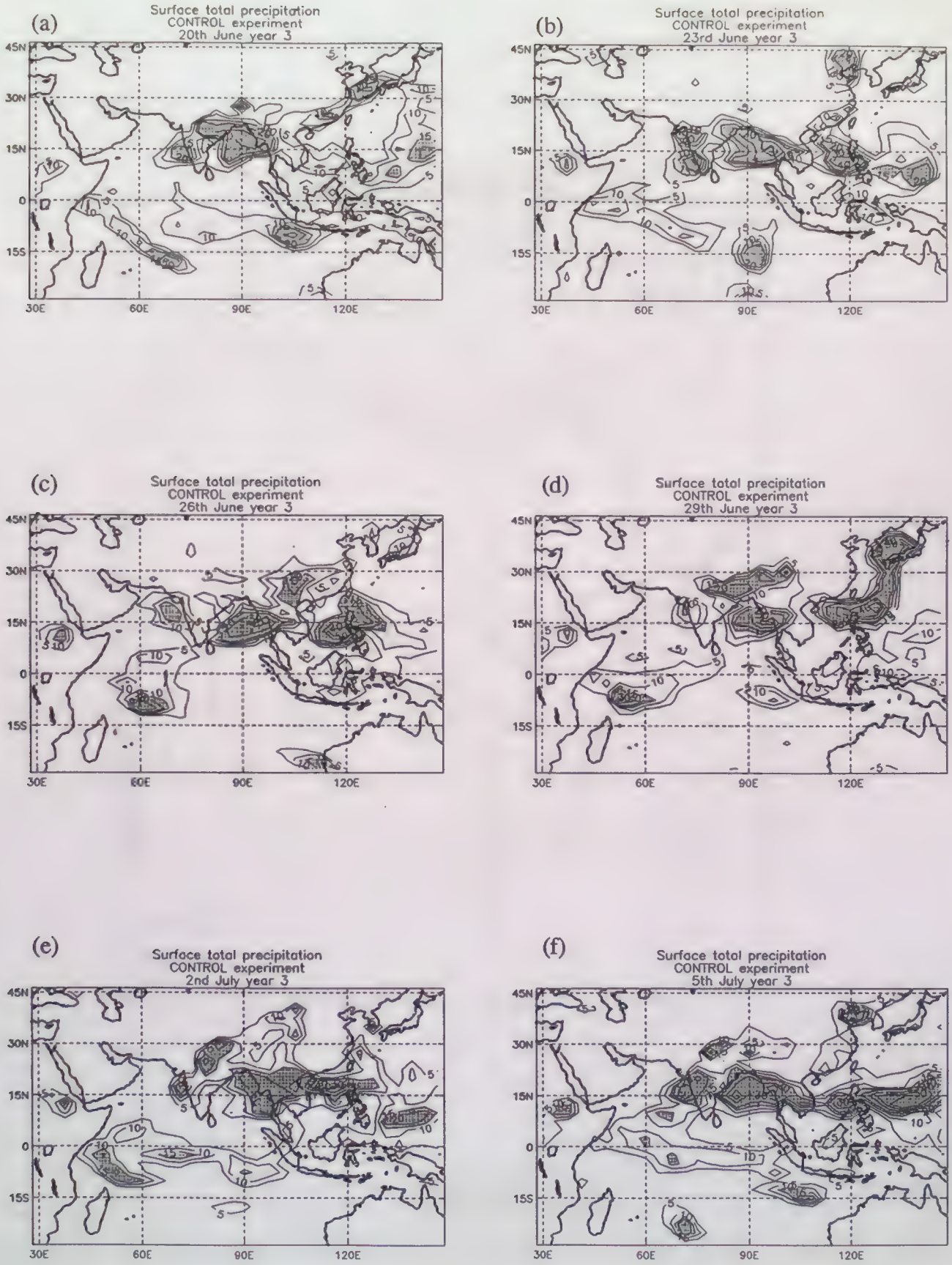
(a)
Surface total precipitation
CONTROL experiment
20th June year 3
(b)
Surface total precipitation
CONTROL experiment
23rd June year 3
(c)
Surface total precipitation
CONTROL experiment
26th June year 3
(d)
Surface total precipitation
CONTROL experiment
29th June year 3
(e)
Surface total precipitation
CONTROL experiment
2nd July year 3
(f)
Surface total precipitation
CONTROL experiment
5th July year 3
45N
30N
15N
0
15S
30E
60E
90E
120E

Figure 11

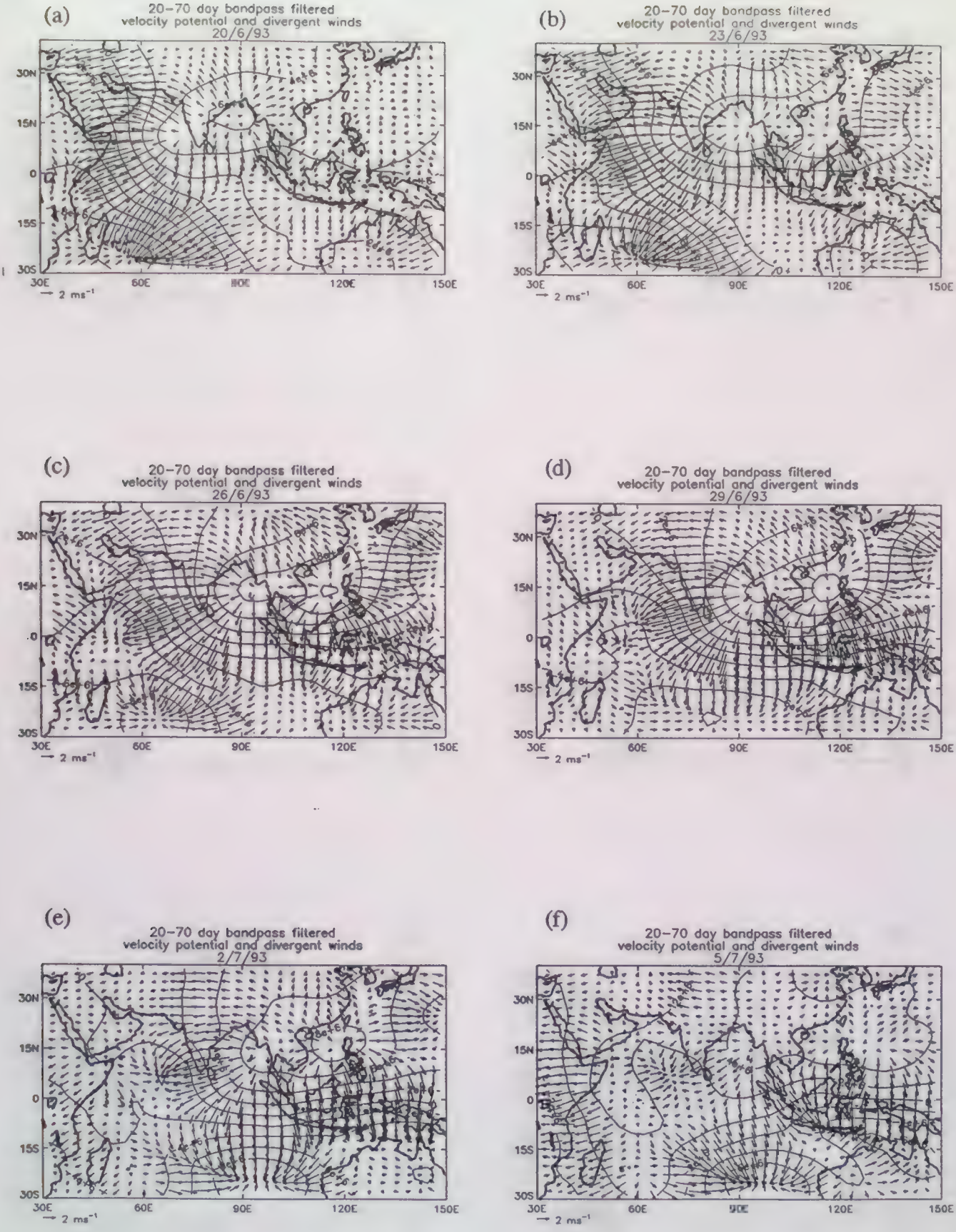
(a)
20–70 day bandpass filtered
velocity potential and divergent winds
20/6/93
(b)
20–70 day bandpass filtered
velocity potential and divergent winds
23/6/93
(c)
20–70 day bandpass filtered
velocity potential and divergent winds
26/6/93
(d)
20–70 day bandpass filtered
velocity potential and divergent winds
29/6/93
(e)
20–70 day bandpass filtered
velocity potential and divergent winds
2/7/93
(f)
20–70 day bandpass filtered
velocity potential and divergent winds
5/7/93
30N
15N
0
15S
30S
30E
60E
90E
120E
150E
2 ms⁻¹

Figure 12

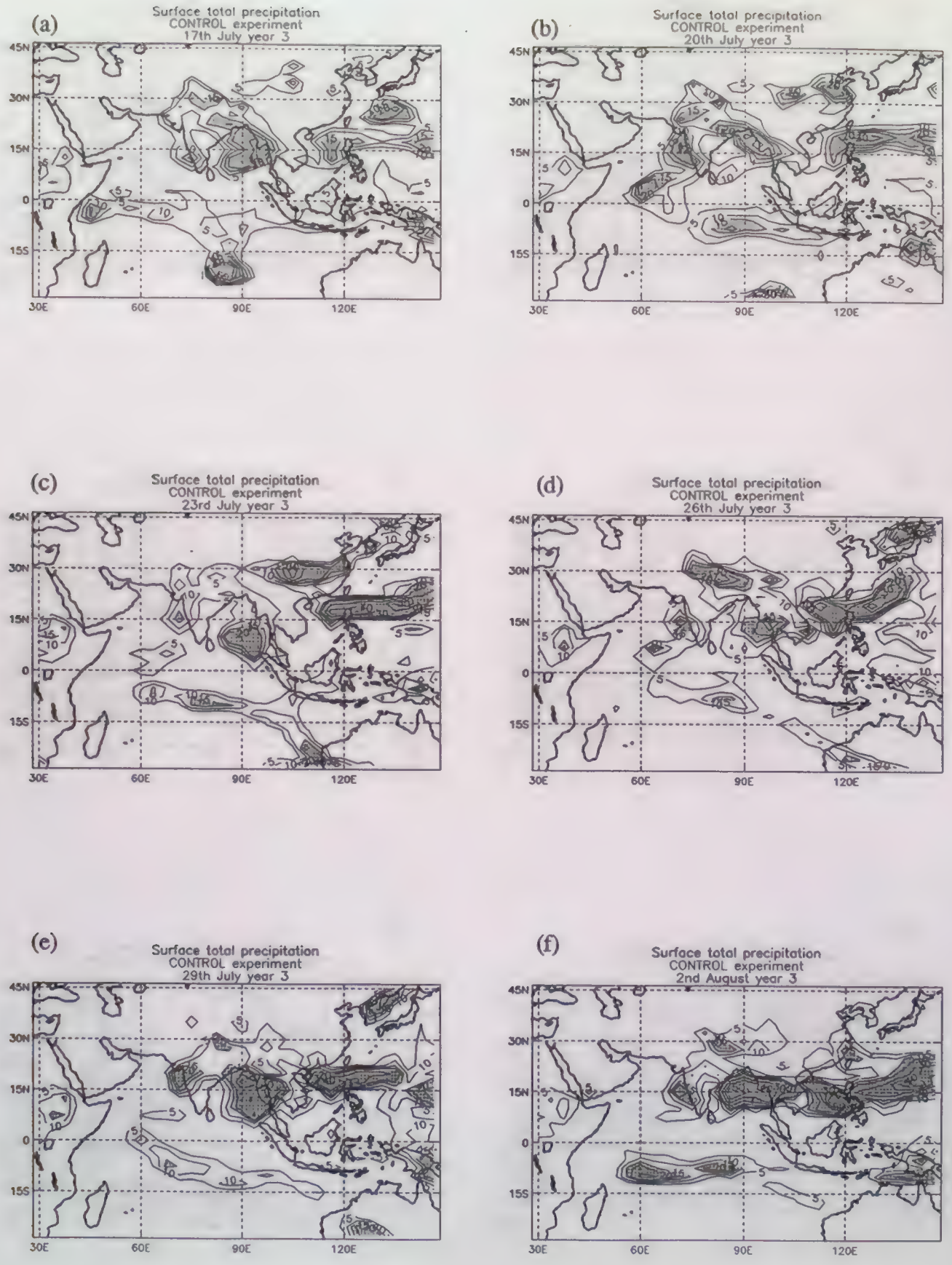
(a)
Surface total precipitation
CONTROL experiment
17th July year 3
(b)
Surface total precipitation
CONTROL experiment
20th July year 3
(c)
Surface total precipitation
CONTROL experiment
23rd July year 3
(d)
Surface total precipitation
CONTROL experiment
26th July year 3
(e)
Surface total precipitation
CONTROL experiment
29th July year 3
(f)
Surface total precipitation
CONTROL experiment
2nd August year 3
45N
30N
15N
0
15S
30E
60E
90E
120E

Figure 13

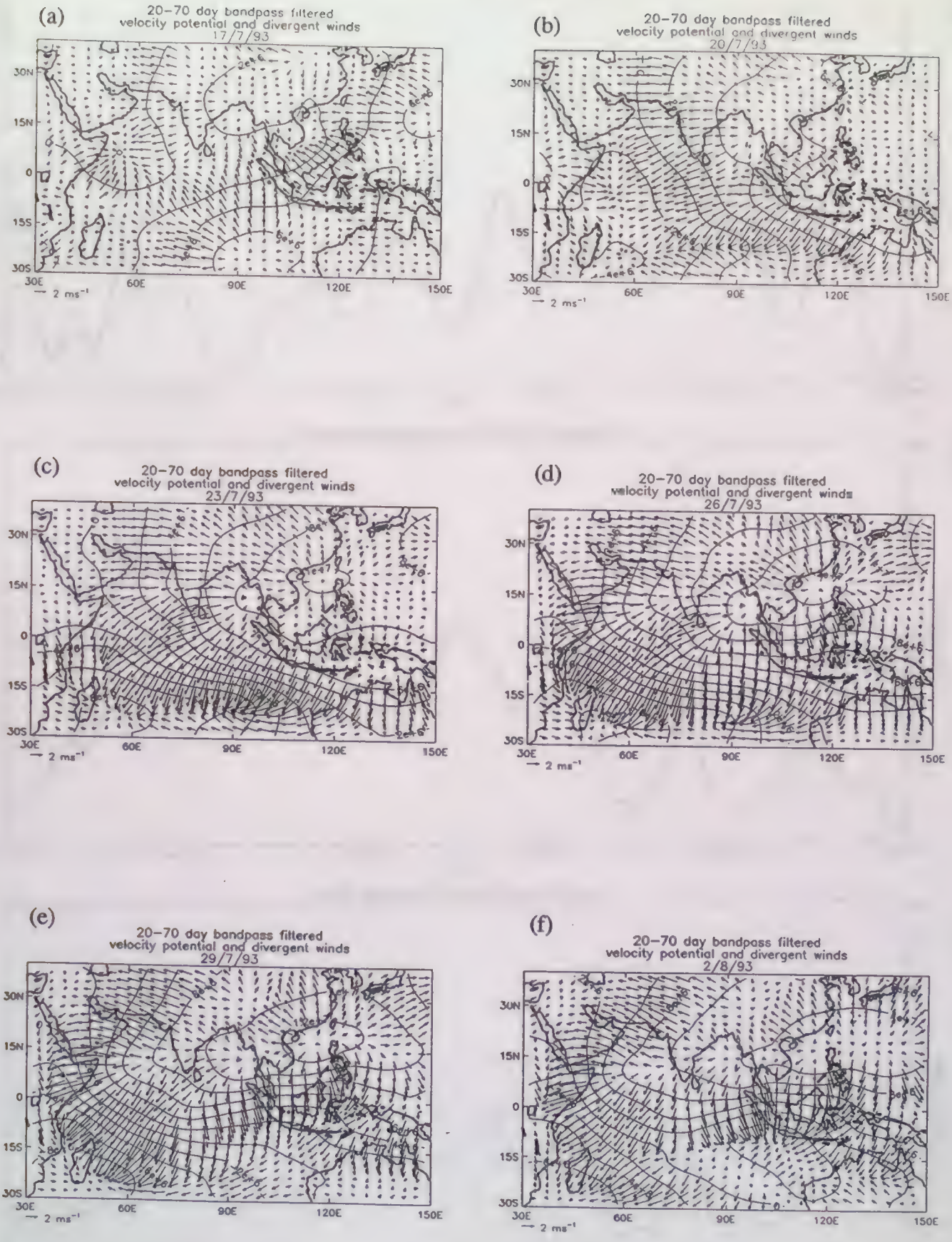
(a)
20–70 day bandpass filtered
velocity potential and divergent winds
17/7/93
(b)
20–70 day bandpass filtered
velocity potential and divergent winds
20/7/93
(c)
20–70 day bandpass filtered
velocity potential and divergent winds
23/7/93
(d)
20–70 day bandpass filtered
velocity potential and divergent winds
26/7/93
(e)
20–70 day bandpass filtered
velocity potential and divergent winds
29/7/93
(f)
20–70 day bandpass filtered
velocity potential and divergent winds
2/8/93
30N
15N
0
15S
30S
30E
60E
90E
120E
150E
2 ms⁻¹

Figure 14

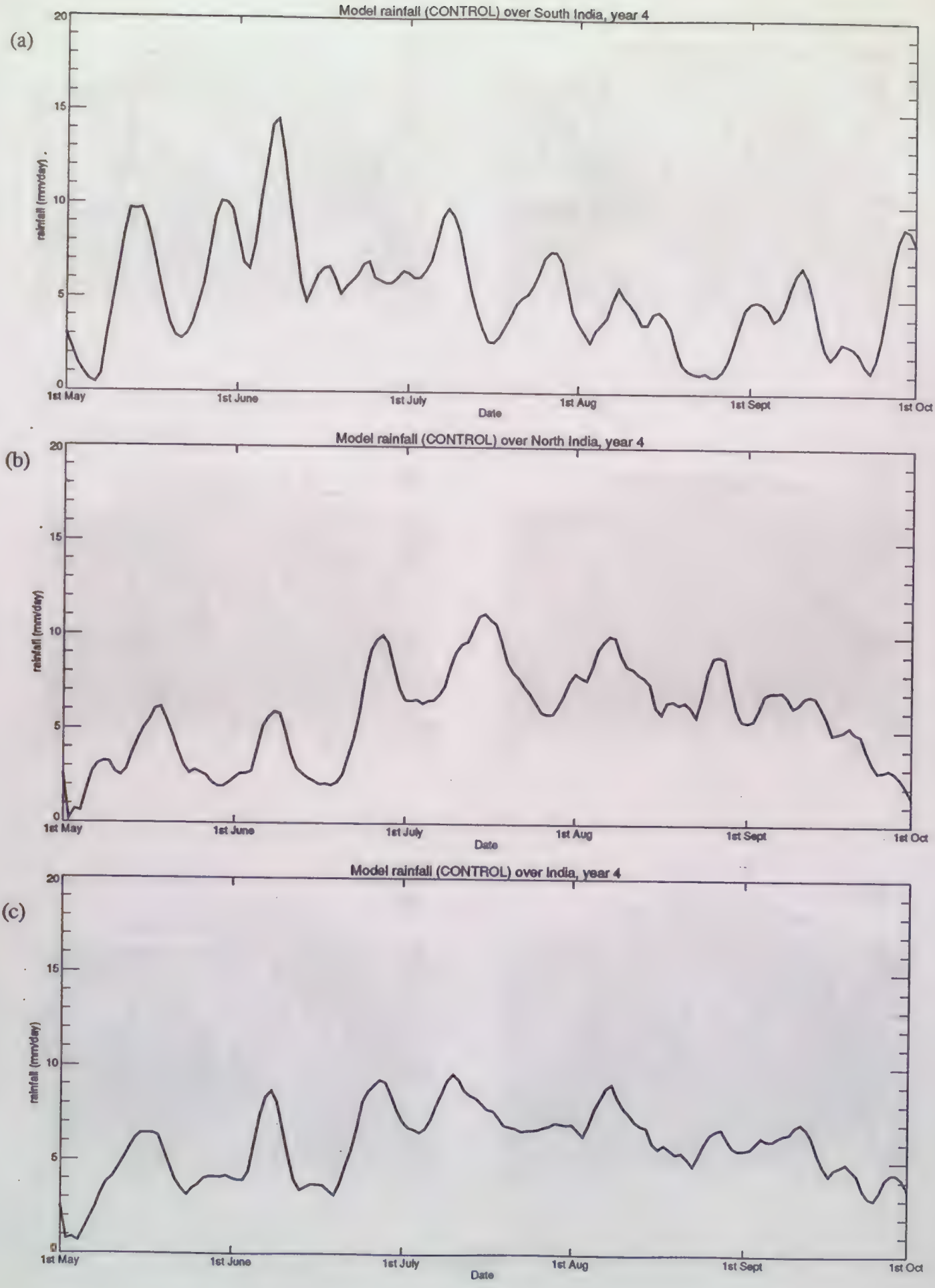
(a)
Model rainfall (CONTROL) over South India, year 4
rainfall (mm/day)
20
15
10
5
0
1st May
1st June
1st July
1st Aug
1st Sept
1st Oct
Date
(b)
Model rainfall (CONTROL) over North India, year 4
rainfall (mm/day)
20
15
10
5
0
1st May
1st June
1st July
1st Aug
1st Sept
1st Oct
Date
(c)
Model rainfall (CONTROL) over India, year 4
rainfall (mm/day)
20
15
10
5
0
1st May
1st June
1st July
1st Aug
1st Sept
1st Oct
Date

Figure 15

(a)

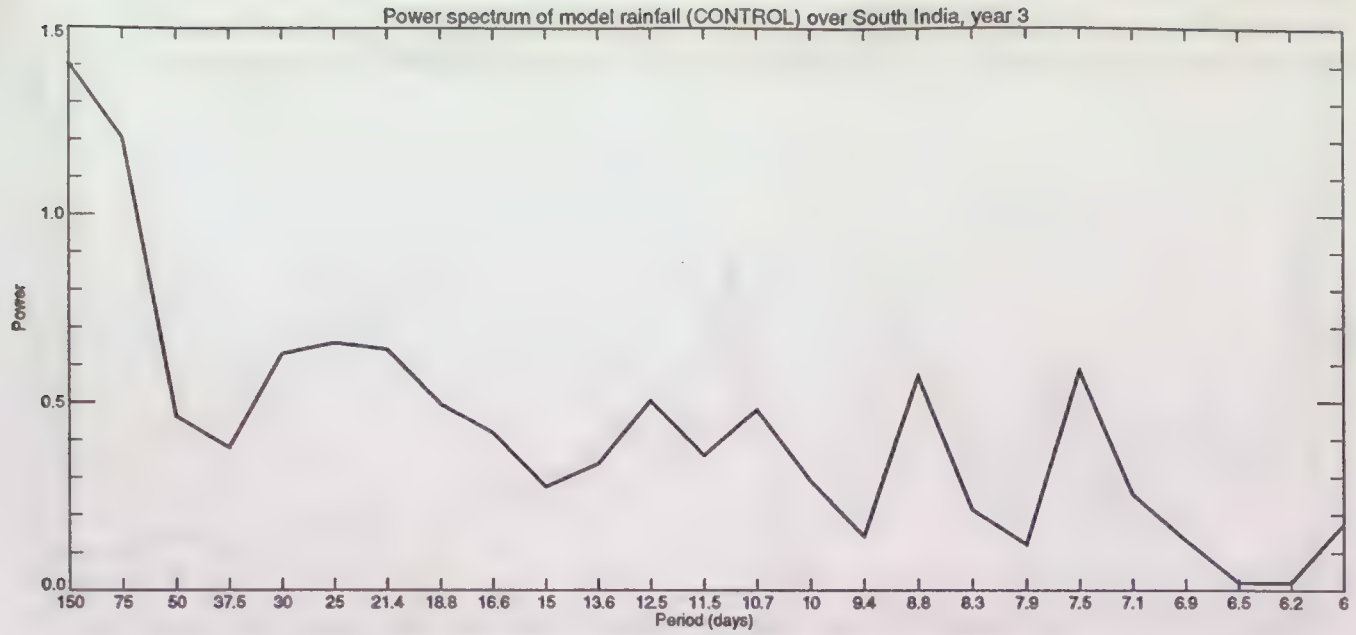

(b)

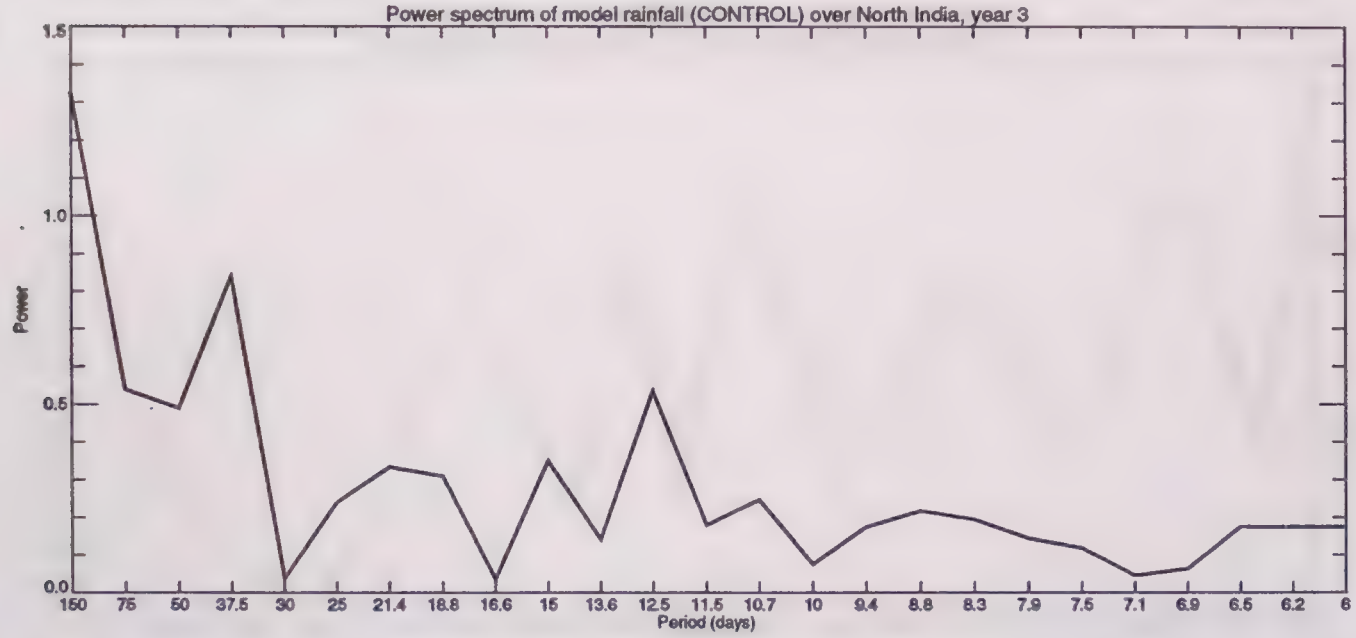

(c)

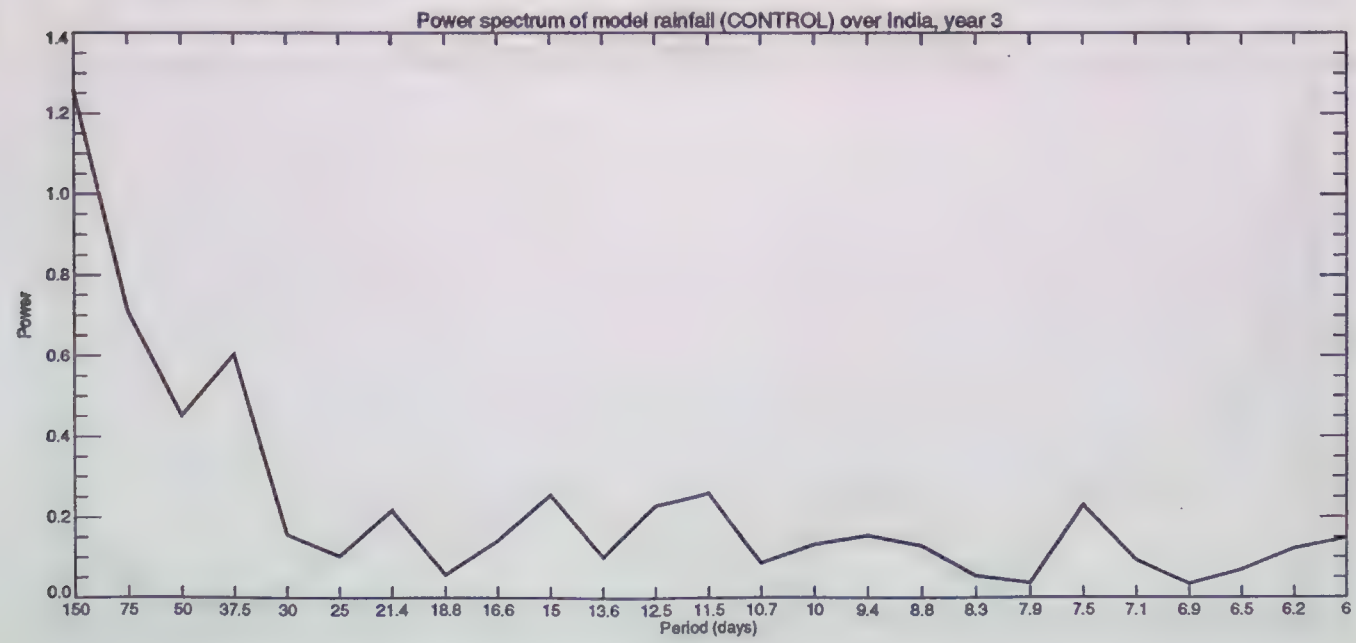

Figure 16(a)

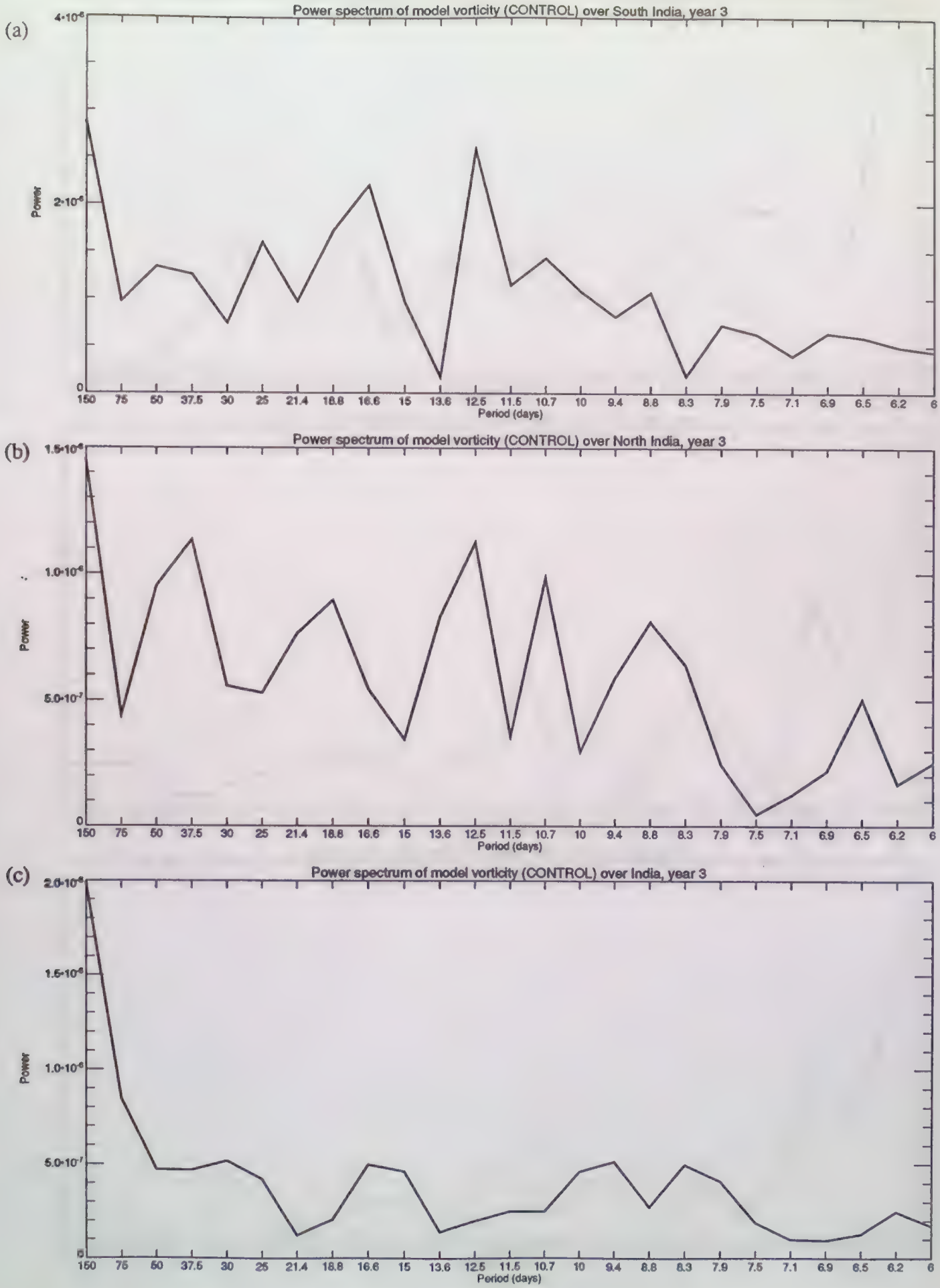
(a)
Power spectrum of model vorticity (CONTROL) over South India, year 3
Power
4·10⁻⁶
2·10⁻⁶
0
150 75 50 37.5 30 25 21.4 18.8 16.6 15 13.6 12.5 11.5 10.7 10 9.4 8.8 8.3 7.9 7.5 7.1 6.9 6.5 6.2 6
Period (days)
(b)
Power spectrum of model vorticity (CONTROL) over North India, year 3
Power
1.5·10⁻⁶
1.0·10⁻⁶
5.0·10⁻⁷
0
150 75 50 37.5 30 25 21.4 18.8 16.6 15 13.6 12.5 11.5 10.7 10 9.4 8.8 8.3 7.9 7.5 7.1 6.9 6.5 6.2 6
Period (days)
(c)
Power spectrum of model vorticity (CONTROL) over India, year 3
Power
2.0·10⁻⁶
1.5·10⁻⁶
1.0·10⁻⁶
5.0·10⁻⁷
0
150 75 50 37.5 30 25 21.4 18.8 16.6 15 13.6 12.5 11.5 10.7 10 9.4 8.8 8.3 7.9 7.5 7.1 6.9 6.5 6.2 6
Period (days)

Figure 16(b)

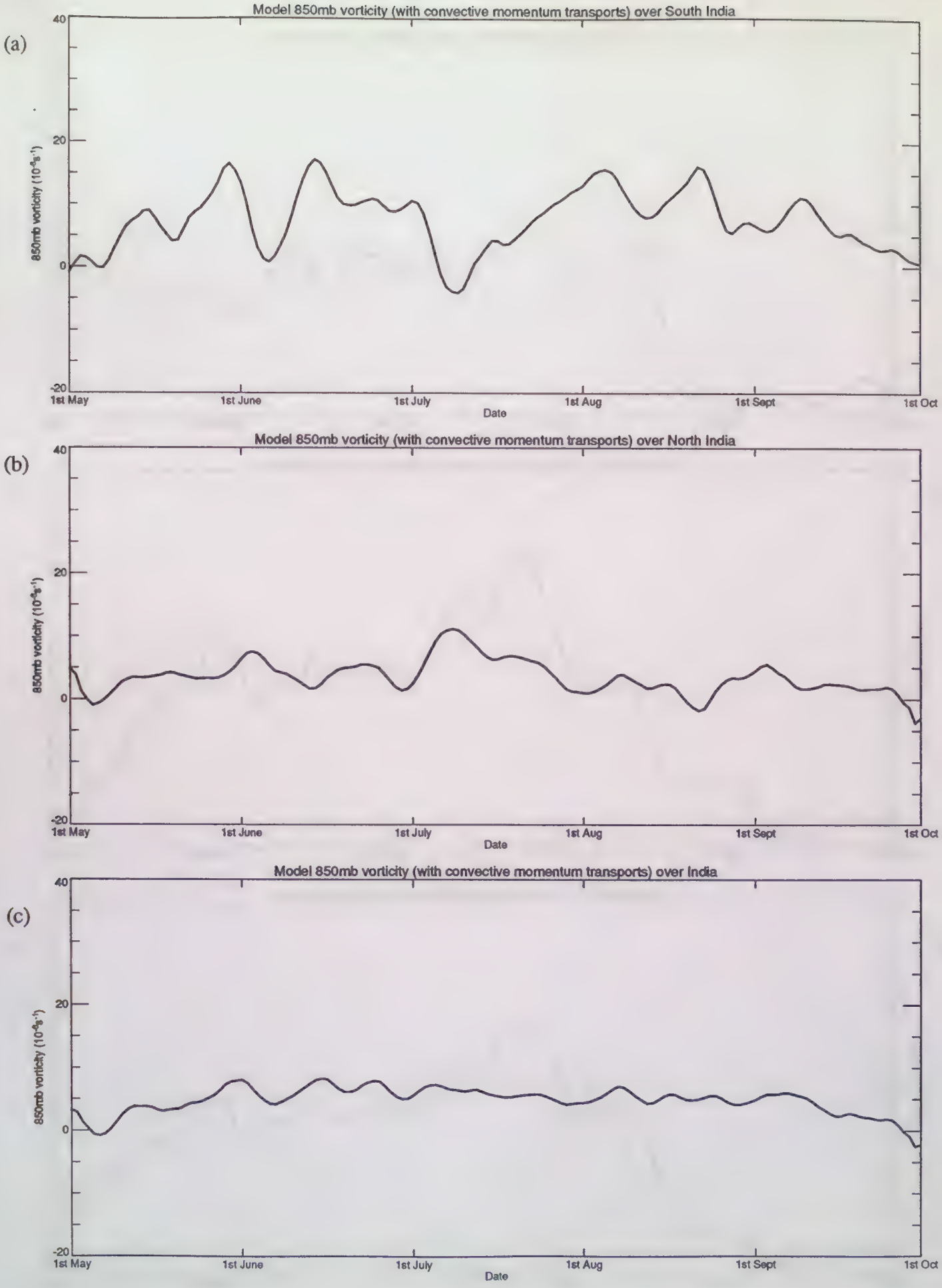
(a)
Model 850mb vorticity (with convective momentum transports) over South India
850mb vorticity ($10^{-6}s^{-1}$)
40
20
0
-20
1st May
1st June
1st July
1st Aug
1st Sept
1st Oct
Date
(b)
Model 850mb vorticity (with convective momentum transports) over North India
850mb vorticity ($10^{-6}s^{-1}$)
40
20
0
-20
1st May
1st June
1st July
1st Aug
1st Sept
1st Oct
Date
(c)
Model 850mb vorticity (with convective momentum transports) over India
850mb vorticity ($10^{-6}s^{-1}$)
40
20
0
-20
1st May
1st June
1st July
1st Aug
1st Sept
1st Oct
Date

Figure 17

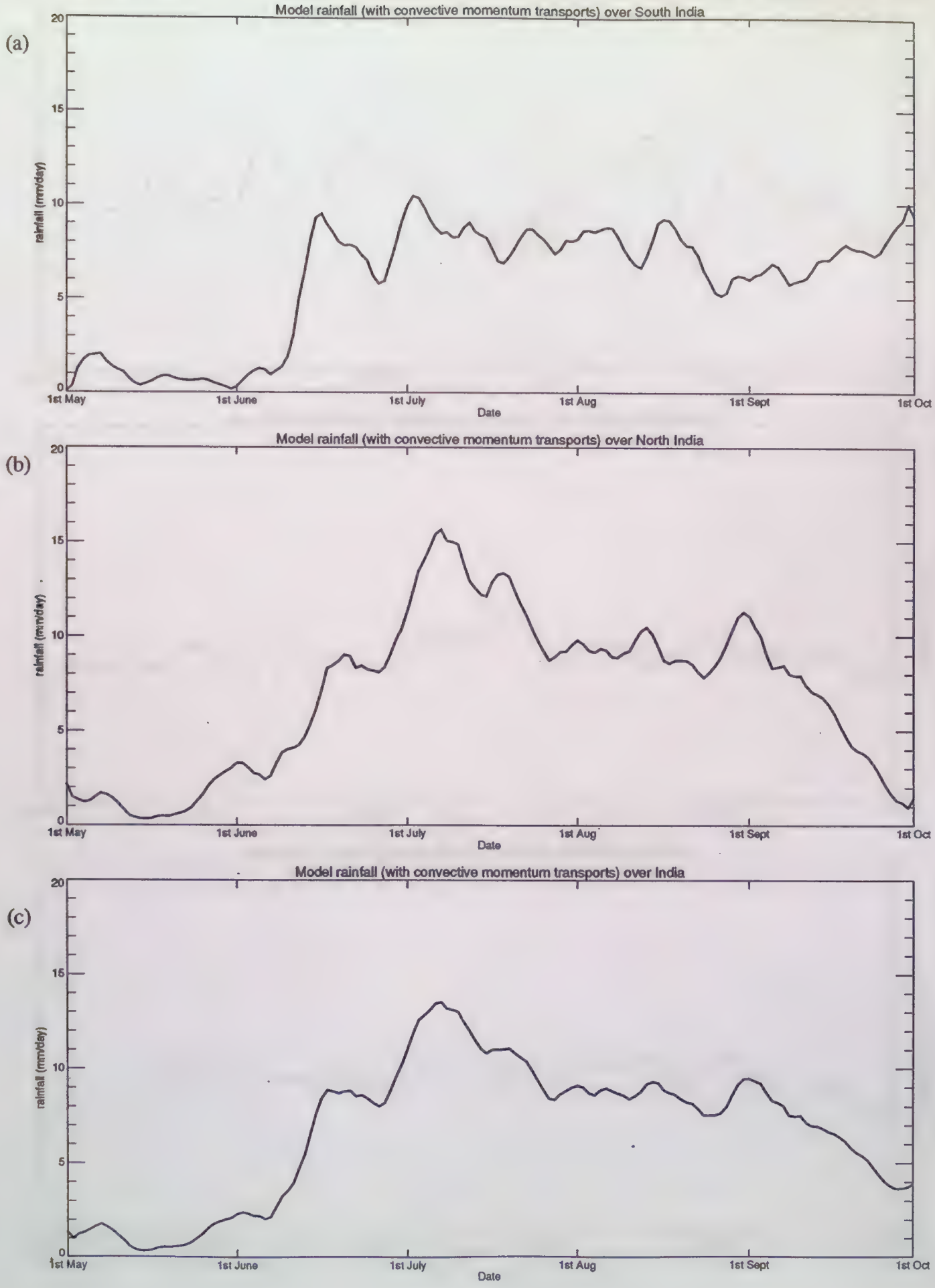
(a)
Model rainfall (with convective momentum transports) over South India
rainfall (mm/day)
0
5
10
15
20
1st May
1st June
1st July
1st Aug
1st Sept
1st Oct
Date
(b)
Model rainfall (with convective momentum transports) over North India
rainfall (mm/day)
0
5
10
15
20
1st May
1st June
1st July
1st Aug
1st Sept
1st Oct
Date
(c)
Model rainfall (with convective momentum transports) over India
rainfall (mm/day)
0
5
10
15
20
1st May
1st June
1st July
1st Aug
1st Sept
1st Oct
Date

Figure 18

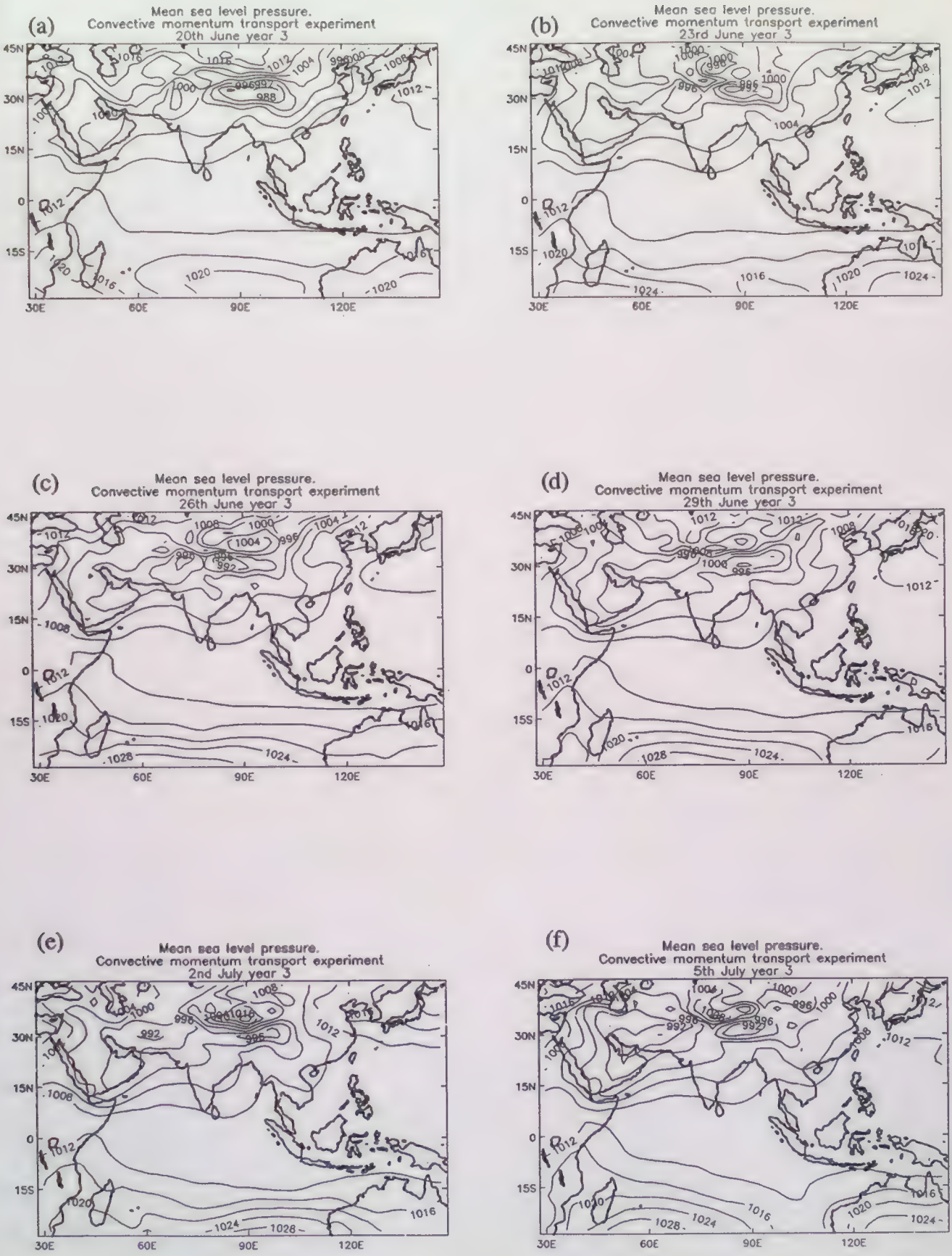
(a)
Mean sea level pressure.
Convective momentum transport experiment
20th June year 3
(b)
Mean sea level pressure.
Convective momentum transport experiment
23rd June year 3
(c)
Mean sea level pressure.
Convective momentum transport experiment
26th June year 3
(d)
Mean sea level pressure.
Convective momentum transport experiment
29th June year 3
(e)
Mean sea level pressure.
Convective momentum transport experiment
2nd July year 3
(f)
Mean sea level pressure.
Convective momentum transport experiment
5th July year 3
45N
30N
15N
0
15S
30E
60E
90E
120E

Figure 19

CLIMATE RESEARCH TECHNICAL NOTES

CRTN 1	Oct 1990	Estimates of the sensitivity of climate to vegetation changes using the Penman-Monteith equation. P R Rowntree
CRTN 2	Oct 1990	An ocean general circulation model of the Indian Ocean for hindcasting studies. D J Carrington
CRTN 3	Oct 1990	Simulation of the tropical diurnal cycle in a climate model. D P Rowell
CRTN 4	Oct 1990	Low frequency variability of the oceans. C K Folland, A Colman, D E Parker and A Bevan
CRTN 5	Dec 1990	A comparison of 11-level General Circulation Model Simulations with observations in the East Sahel. K Maskell
CRTN 6	Dec 1990	Climate Change Prediction. J F B Mitchell and Qing-cun Zeng
CRTN 7	Jan 1991	Deforestation of Amazonia - modelling the effects of albedo change. M F Mylne and P R Rowntree
CRTN 8	Jan 1991	The role of observations in climate prediction and research. D J Carson
CRTN 9	Mar 1991	The greenhouse effect and its likely consequences for climate change. D J Carson
CRTN 10	Apr 1991	Use of wind stresses from operational N.W.P. models to force an O.G.C.M. of the Indian Ocean. D J Carrington
CRTN 11	Jun 1991	A new daily Central England Temperature series, 1772-1991. D E Parker, T P Legg and C K Folland
CRTN 12	Jul 1991	Causes and predictability of Sahel rainfall variability. D P Rowell, C K Folland, K Maskell, J A Owen, M N Ward

CLIMATE RESEARCH TECHNICAL NOTES

CRTN 13	Jul 1991	Modelling changes in climate due to enhanced CO2, the role of atmospheric dynamics, cloud and moisture. C A Senior, J F B Mitchell, H Le Treut and Z-X Li
CRTN 14	Sep 1991	Sea temperature bucket models used to correct historical SST data in the Meteorological Office. C K Folland
CRTN 15	Aug 1991	Modelling climate change, and some potential effects on agriculture in the U.K. P R Rowntree, B A Callander and J Cochrane
CRTN 16	Aug 1991	The Boreal Forests and Climate G Thomas and P R Rowntree
CRTN 17	Aug 1991	Development of a Stratosphere-Troposphere Data Assimilation System. R Swinbank.
CRTN 18	Sep 1991	A study of asynchronous coupling using a simple climate model. M K Davey.
CRTN 19	Sep 1991	The Oceanic Carbon Cycle. N K Taylor
CRTN 20	Nov 1991	Worldwide ocean-atmosphere surface fields in Sahel wet and dry years using provisionally corrected surface wind data. M N Ward
CRTN 21	Dec 1991	Coupled tropical ocean global atmosphere models at the UKMO. M K Davey, C Gordon, S Ineson and S Lawrence
CRTN 22	Dec 1991	Empirical parameterisation of tropical ocean-atmosphere coupling. M Allen, M K Davey, D L T Anderson and P D Killworth
CRTN 23	Feb 1992	The temporal evolution of Equatorial Currents in the Indian Ocean D L T Anderson, D J Carrington, R A Corry and C Gordon
CRTN 24	Feb 1992	Stratospheric analyses provided by the U.K. Meteorological Office M J Bailey, A O'Neill and V D Pope

CLIMATE RESEARCH TECHNICAL NOTES

CRTN 25	Feb 1992	Modelling interannual variability in the Indian Ocean using momentum fluxes from the UKMO and ECMWF operational weather analyses. D L T Anderson and D J Carrington
CRTN 26	Mar 1992	A GCM simulation of the impact of Amazonian deforestation on climate using an improved canopy representation J Lean and P R Rowntree
CRTN 27	Mar 1992	The parameterization of rainfall interception in GCMs A J Dolman and D Gregory
CRTN 28	Jun 1992	Development of worldwide marine data eigenvectors since 1985 A W Colman
CRTN 29	Jun 1992	A tropical ocean model with reduced physics M K Davey
CRTN 30	Jun 1992	International Temperature Workshop, Boulder, Colorado, USA, 16 January 1992 Edited by D E Parker
CRTN 31	Jul 1992	Simulation of clear-sky outgoing longwave radiation over the oceans using operational analyses A Slingo and M J Webb
CRTN 32	Sep 1992	A prediction of the transient response of climate J M Murphy
CRTN 33	Nov 1992	LEPS scores for assessing climate model simulations and long-range forecasts. C K Folland
CRTN 34	Jan 1993	Stratospheric Data Assimilation System Guide Editer: R Swinbank
CRTN 35	Mar 1993	A Stratosphere-Troposphere Data Assimilation System R Swinbank and A O'Neill
CRTN 36	Mar 1993	Validation of hydrological schemes for climate models against catchment data. P R Rowntree and J Lean

CLIMATE RESEARCH TECHNICAL NOTES

CRTN 37	Apr 1993	Modelling of palaeoclimates: Examples from the recent past J F B Mitchell
CRTN 38	May 1993	A simulation of seasonality in ENSO forecast skill M K Davey, D L T Anderson and S Lawrence
CRTN 39	Jul 1993	ENSO Prediction experiments using a simple ocean-atmosphere model D-H Wu, D L T Anderson and M K Davey
CRTN 40	Sep 1993	Diagnosis of dynamic sea-surface and sea-level changes from the Cox ocean model J M Gregory
CRTN 41	Sep 1993	Seasonal variations of the clear-sky greenhouse effect: the role of changes in atmospheric temperatures and humidities M J Webb, A Slingo and G L Stephens
CRTN 42	Nov 1993	Sea-level changes under increasing atmospheric CO_2 in a transient coupled ocean-atmosphere GCM experiment. J M Gregory
CRTN 43	Dec 1993	Global and regional patterns of climate change: recent predictions for the Arctic P R Rowntree
CRTN 44	Feb 1994	The effect of changing horizontal diffusion in the atmospheric version of the unified climate model C D Hall and R A Stratton
CRTN 45	Mar 1994	Simulation of El-Niño/Southern Oscillation like variability in a global AOGCM and its response to CO_2 increase. S F B Tett
CRTN 46	Apr 1994	Global data required for monitoring climate change. D E Parker and C K Folland
CRTN 47	May 1994	Seasonal uptake of anthropogenic CO_2 in an ocean general circulation model. N K Taylor

CLIMATE RESEARCH TECHNICAL NOTES

CRTN 48	Jun 1994	A tropic-wide oscillation of boreal summer rainfall and patterns of sea-surface temperature. M N Ward, K Maskell, C K Folland, D P Rowell and R Washington
CRTN 49	Jun 1994	Simulation of the tropical Pacific using a simplified ocean model M A Balmaseda, D L T Anderson and M K Davey
CRTN 50	Sep 1994	Simulation of global mean temperature using a box-diffusion climate model P R Rowntree
CRTN 51	Sep 1994	Seasonal dependence of ENSO prediction skill M A Balmaseda, M K Davey and D L T Anderson
CRTN 52	Nov 1994	Simulation of the Indian Monsoon and Tropical Intraseasonal Variability by a General Circulation Model P M Inness and D Gregory
CRTN 53	Mar 1995	A comparison of modelled surface fluxes with climatological estimates. C Gordon and D K Wright
CRTN 54	Mar 1995	The representation of moist convection in atmospheric models. D Gregory
CRTN 55	Mar 1995	A consistent treatment of the evaporation of rain and snow for use in large-scale models D Gregory
CRTN 56	Apr 1995	Workshop on simulations of the Climate of the Twentieth Century using GISST, 28-30 November 1994, Hadley Centre, Bracknell, UK Edited by C K Folland and D P Rowell
CRTN 57	May 1995	Enhanced shortwave cloud radiative forcing due to anthropogenic aerosols. S E Swartz and A Slingo
CRTN 58	May 1995	The simulation of the tropical oceans in models of different horizontal resolution. C Gordon, D K Wright and C M Roberts
CRTN 59	Sep 1995	The water budget of middle latitude continental regions - a modelling and observational study P R Rowntree
CRTN 60	Sep 1995	Intraseasonal variability of the Indian summer monsoon simulated by the Hadley Centre climate model K Ashok, D Gregory and P M Inness